Marine and Petroleum Geology 66 (2015) 764–790

Contents lists available at ScienceDirect

Marine and Petroleum Geology

journal homepage: www.elsevier.com/locate/marpetgeo

Research paper

Composition of the Lower Cretaceous source rock from the Austral Basin (Río Mayer Formation, Patagonia, Argentina): Regional implication for unconventional reservoirs in the Southern Andes

Sebastián Richiano [a, b, *], Augusto N. Varela [a, b], Lucía E. Gómez-Peral [a, b], Abril Cereceda [a, b], Daniel G. Poiré [a, b]

[a] Centro de Investigaciones Geológicas, Universidad Nacional de La Plata-CONICET, calle 1Nº 644 (1900) La Plata, Argentina
[b] Cátedras de Sedimentología y Rocas sedimentarias, Universidad Nacional de La Plata, calle 60 y 122 s/n, La Plata, Argentina

ARTICLE INFO

Article history:
Received 8 January 2014
Received in revised form
17 July 2015
Accepted 19 July 2015
Available online 22 July 2015

Keywords:
Clay assemblages
Petrographic analysis
SEM-EDAX
Shale-oil/gas

ABSTRACT

The importance of the Río Mayer Formation (Lower Cretaceous, prodelta to marine outer shelf) in the hydrocarbon development of the Austral Basin (Patagonia, Argentina) has been recognized by several authors. This unit plays a key-role as source rock and caprock in the "Inoceramus inferior-Springhill" petroleum system, the most important in the basin. In this work we demonstrate that the composition of the Río Mayer Formation highly matches with the requirements to be considered for shale-oil/gas exploitation. The unit studied mainly consists of laminated black siliciclastic mudtones and shales with interbedded marlstones and sandstone levels, and in subsurface shows TOC values up to 3% and kerogen types between II and III. Compositional studies from outcrops of this unit are almost absent and constitute the main focus of this contribution. A total of ten detailed sedimentological logs were measured from the field and X-ray diffraction analysis (XRD), standard petrography, scanning electron microscopy (SEM) and determination of major elements in clay minerals by EDAX were carried out in order to characterize the composition of the Río Mayer Formation. XRD analyses (in fine-grained sediments) indicate a composition dominated by quartz and calcite, with minor proportions of feldspars and clays. Marine sediments are dominated by illite and chlorite, and commonly accompanied by mixed layered illite-smectite (IS), while the prodelta is smectite-dominated with more than 90% of this clay. Both, authigenic and detrital clays were identified using SEM-EDAX. Sandstones of the Río Mayer Formation are generally lithic and feldspar graywackes. Provenance analyses in sandstones make possible the discrimination of four groups of samples differentiated by their ages and palaeoenvironments. In comparison with other important shale-reservoirs from North America (Barnett, Marcellus, Woodford, Haynesville and Doig), the composition of the unit studied have more quartzitic composition, reflecting in a high brittleness index (BI) that result in a clear brittle pattern.

1. Introduction

Compositional studies are often useful for analysing the evolution of sedimentary basins, revealing temporal and space variations in the participation of different sediment source areas, tectonic settings and degree of diagenesis, among others (Dickinson and Rich, 1972; Ingersoll, 1983; Critelli and Ingersoll, 1995; Inglès and Ramos-Guerrero, 1995; Cavazza and Ingersoll, 2005; Do Campo et al., 2010; Gómez-Peral et al., 2011; Varela et al., 2013). Traditionally, for oil-basins, these kinds of studies were developed in the sandstone reservoirs, particularly the provenance analysis (quantitative petrography, heavy mineral analysis, mineral chemistry and isotopic determinations) (De Rossi Fontanelli et al., 2012). There are examples of provenance analysis as a tool for many different aspects in oil-exploration, such as an alternative method for reservoir correlation, for the analysis of sedimentary dispersal patterns, for the definition and modelling of reservoir geometry, and for the

* Corresponding author. Centro de Investigaciones Geológicas, Universidad Nacional de La Plata-CONICET, calle 1Nº 644 (1900) La Plata, Argentina.
E-mail addresses: richiano@cig.museo.unlp.edu.ar (S. Richiano), augustovarela@cig.museo.unlp.edu.ar (A.N. Varela), lperal@cig.museo.unlp.edu.ar (L.E. Gómez-Peral), acereceda@cig.museo.unlp.edu.ar (A. Cereceda), poire@cig.museo.unlp.edu.ar (D.G. Poiré).

http://dx.doi.org/10.1016/j.marpetgeo.2015.07.018
0264-8172/

recognition of diagenetic patterns (Morton, 1987; Hurst and Morton, 1988; Allen and Mange-Rajetzky, 1992; Mearns, 1992; Morton and Hallsworth, 1994; Morton et al., 2002, 2003, 2005; Rossi et al., 2002; De Rossi Fontanelli et al., 2012). In recent years the investigations of fine sediments have increased dramatically mainly since compositional studies are using for the mineralogical and petrophysical characterization of unconventional resources (Chalmers et al., 2012; Hammes and Frébourg, 2012; Kohl et al., 2014; among others).

For the Austral Basin (Santa Cruz province, Patagonia Argentina) few compositional papers are only registered, most of them developed in sandstones (Manassero, 1988; Macellari et al., 1989; Spalletti et al., 2006; Varela et al., 2013) and one work that only refer the fine sediments (Iñiguez Rodriguez and Decastelli, 1984). This work constitutes the first outcrop compositional study of the Lower Cretaceous Río Mayer Formation in the Austral Basin based on X-ray diffraction (XRD), standard petrography and SEM-EDAX of fine sediments (siliciclastic mudstones, shales and marlstones) combined with standard petrography of sandstones.

The importance of the Río Mayer Formation in the hydrocarbon development of the Austral Basin has been recognized long ago by several authors (Pittion and Gouadain, 1992; Pittion and Arbe, 1999; Rodríguez and Cagnolatti, 2008; Belotti et al., 2013; Zanella et al., 2013). This unit is considered as source rock and caprock in the "Inoceramus inferior-Springhill" petroleum system, which is the best documented and which has expelled large quantities of oil to the basin (Rodríguez and Miller, 2005; Argüello et al., 2005). The Río Mayer Formation is a proven hydrocarbon source rock with high TOC content ranging between 0.5 and 3%, kerogen types II and III and diagenetic conditions place it in the oil window in the study area (Rodríguez and Cagnolatti, 2008; Legarreta and Villar, 2011; Richiano, 2012; Richiano et al., 2012; Belotti et al., 2013; Richiano, 2014). The important thickness and its wide areal distribution over the basin, together with the characteristics mentioned above, indicate that this unit possesses all the attributes needed to join the new exploratory horizon in South America, the shale-oil/gas paradigm.

The aim of this contribution is to provide original compositional data of the mudstones and shales (detrital and authigenic components); and the sandstones provenance of the Lower Cretaceous Río Mayer Formation in the Austral Basin. Shale plays are geologically much more complicated than typically described (Binnion, 2012), so the detailed analyses here presented constitute a powerful tool for a better mineralogical definition of unconventional resources. Furthermore, it provides highly valuable information in the interpretation of the factors controlling the evolution of this basin and in particular the development of the hydrocarbon source rocks.

2. Geological background

The Austral Basin is located in the South-western Patagonia and constitutes one of the most important oil-basins in Argentina, having a maximum thickness of 8000 m in the subsurface with excellent thermal maturity (Fig. 1A–B). The geological history of the Austral Basin in the study area is characterized by three main tectonic stages (Biddle et al., 1986; Rodríguez and Miller, 2005; Varela et al., 2012), a rift stage, a stage of thermal subsidence and, finally, a foreland stage.

Rift Stage (Middle Jurassic–earliest Cretaceous): In the Andean Cordillera is recognized as El Quemado Complex, Ibañez and Tobífera formations (Biddle et al., 1986; Pankhurst et al., 2000). In this initial stage, grabens and half-grabens were developed and filled with volcaniclastic and volcanic rocks intercalated with some epiclastic sediments (Biddle et al., 1986).

Thermal Subsidence Stage (Berriasian to Albian): Once the tectonic activity had ceased and thermal subsidence stage began, the characteristic continental to shallow marine transgressive succession of the Springhill Formation was deposited. The Springhill Formation broadly overlaps the margins of the initial half-graben, and it is overlain by a thick marine succession, characterized by alternating black mudstones, shales and marlstones of the Río Mayer Formation, which extends to the Albian (Richiano, 2012; Richiano et al., 2012). Towards the end of this stage (early Aptian – Albian), a large passive-margin delta system, recorded in the Piedra Clavada Formation, developed in the northern and eastern sectors of the basin.

Foreland Stage (Albian/Cenomanian to recent): A regional change from extensional to shortening deformation took place in the Late Cretaceous and shortening continued to the Neogene (Biddle et al., 1986; Wilson, 1991; Spalletti and Franzese, 2007; Fosdick et al., 2011). The shortening associated with the early stages of the orogeny caused the development of a retroarc fold-and-thrust belt along the Patagonian–Fueguian Andes (Biddle et al., 1986; Fildani et al., 2003; Fildani and Hessler, 2005; Fosdick et al., 2011; Varela et al., 2012). This fold-and-thrust belt is associated along its eastern margin with a foreland basin (Austral Foreland Basin/Magallanes Basin). The onset of the shortening phase in the northern sector of the Austral Basin took place about 100 Ma ago and it is characterized by the west to east progradation of the fluvial-estuarine facies of the Mata Amarilla Formation (Varela, 2011; Varela et al., 2012).

The Río Mayer Formation was deposited during the *sag* stage of the Austral Basin, it is composed of siliciclastic mudstones, shales and marlstones interbedded with scarce fine-grained sandstones deposited in fully marine shelf environments. It overlies the El Quemado Complex in paraconcordance and the Springhill Formation in concordance or paraconcordance (Kraemer and Riccardi, 1997). In the study area the upper limit of the unit shows a transitional pattern with two formations: to the north, the Piedra Clavada Formation (=Kachaike) and the Cerro Toro Formation towards the south (Riccardi, 1968, 1971; Riccardi and Rolleri, 1980; Arbe and Hechem, 1984; Kraemer and Riccardi, 1997; Marinelli, 1998; Richiano et al., 2012) (Fig. 2). The Río Mayer Formation in the subsurface stratigraphy partially matches with the Lower and Middle Palermo Aike Formation (Fig. 2).

At the Seccional Río Guanaco locality (Fig. 1) the Río Mayer Formation was divided in three informal sections from a sedimentological point of view (Fig. 3; Richiano et al., 2012). The lower section is mainly composed of laminated black shales with both tabular and concretional marlstone levels. Trace fossils were not observed in this section, but ammonites and belemnites are abundant. The high proportion of fine sediments containing an open marine fauna suggests that the lower section was accumulated in an outer shelf setting (Richiano et al., 2012). Two fossiliferous levels were recorded by Kraemer and Riccardi (1997) assigned to this section, corresponding to early Berrasian and early Valanginian ages. TOC values from this section ranging between 0.07 and 2.81% (Richiano, 2014).

The middle section has 40 m thickness and is composed of intensely bioturbated black marlstones and siliciclastic mudstones. This section is characterized by the *Zoophycos* ichnofacies consisting of *Bergaueria*, *Chondrites* and *Zoophycos* ichnogenera (Richiano et al., 2013; Richiano, 2015). Body fossils are common, especially belemnites. These fossils represent a Belemnopsis fauna that correspond to Valanginian-Hauterivian age (Aguirre Urreta, 2002; Richiano, 2012). In this section TOC values are from 0.07 to 0.58% (Richiano, 2014).

Finally, the upper section (Hauterivian–Albian) reach 150–200 m of thickness, it is characterized by massive black siliciclastic mudstones with intercalations of very fine-to fine-grained

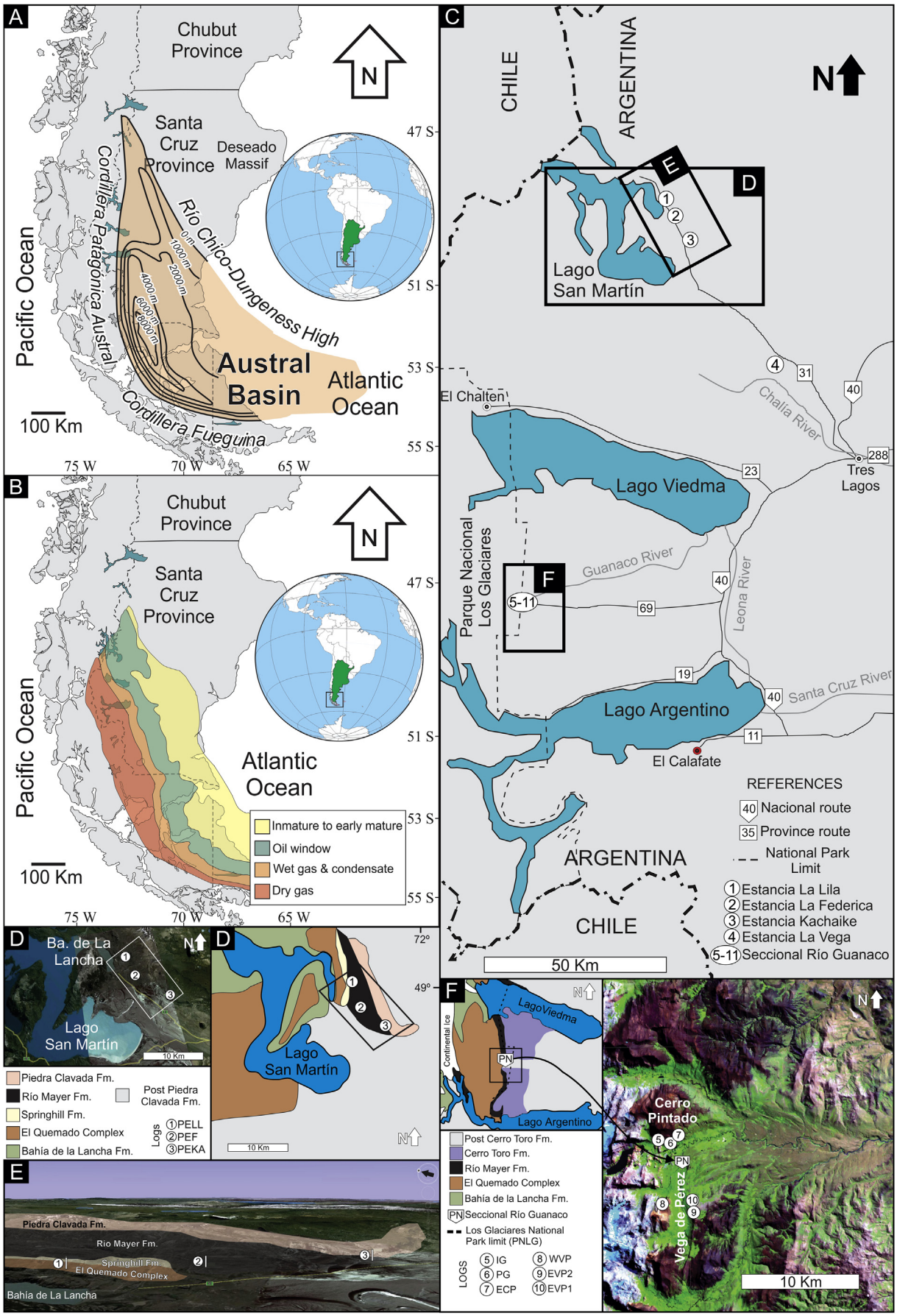
A
Chubut Province
Santa Cruz Province
Deseado Massif
Cordillera Patagónica Austral
Río Chico-Dungeness High
0 m
1000 m
2000 m
4000 m
6000 m
8000 m
Austral Basin
Atlantic Ocean
Pacific Ocean
Cordillera Fueguina
100 Km
47 S
51 S
53 S
55 S
75 W
70 W
65 W
N
B
Chubut Province
Santa Cruz Province
Pacific Ocean
Atlantic Ocean
Inmature to early mature
Oil window
Wet gas & condensate
Dry gas
100 Km
47 S
51 S
53 S
55 S
75 W
70 W
65 W
N
C
CHILE
ARGENTINA
N
E
D
Lago San Martín
1
2
3
4
31
40
El Chalten
Chalía River
288
Tres Lagos
23
Lago Viedma
Parque Nacional Los Glaciares
F
5-11
Guanaco River
69
40
Leona River
19
Lago Argentino
40
Santa Cruz River
11
El Calafate
ARGENTINA
CHILE
50 Km
REFERENCES
40 Nacional route
35 Province route
National Park Limit
1 Estancia La Lila
2 Estancia La Federica
3 Estancia Kachaike
4 Estancia La Vega
5-11 Seccional Río Guanaco
D
Ba. de La Lancha
Lago San Martín
10 Km
N
Piedra Clavada Fm.
Río Mayer Fm.
Springhill Fm.
El Quemado Complex
Bahía de la Lancha Fm.
Post Piedra Clavada Fm.
Logs
1 PELL
2 PEF
3 PEKA
D
72°
49°
Lago San Martín
10 Km
N
F
Continental Ice
LagoViedma
PN
Lago Argentino
N
Post Cerro Toro Fm.
Cerro Toro Fm.
Río Mayer Fm.
El Quemado Complex
Bahía de la Lancha Fm.
PN Seccional Río Guanaco
Los Glaciares National Park limit (PNLG)
LOGS
5 IG
6 PG
7 ECP
8 WVP
9 EVP2
10 EVP1
N
Cerro Pintado
5
6
7
PN
8
10
9
Vega de Pérez
10 Km
E
Piedra Clavada Fm.
Río Mayer Fm.
Springhill Fm.
El Quemado Complex
Bahía de La Lancha
1
2
3

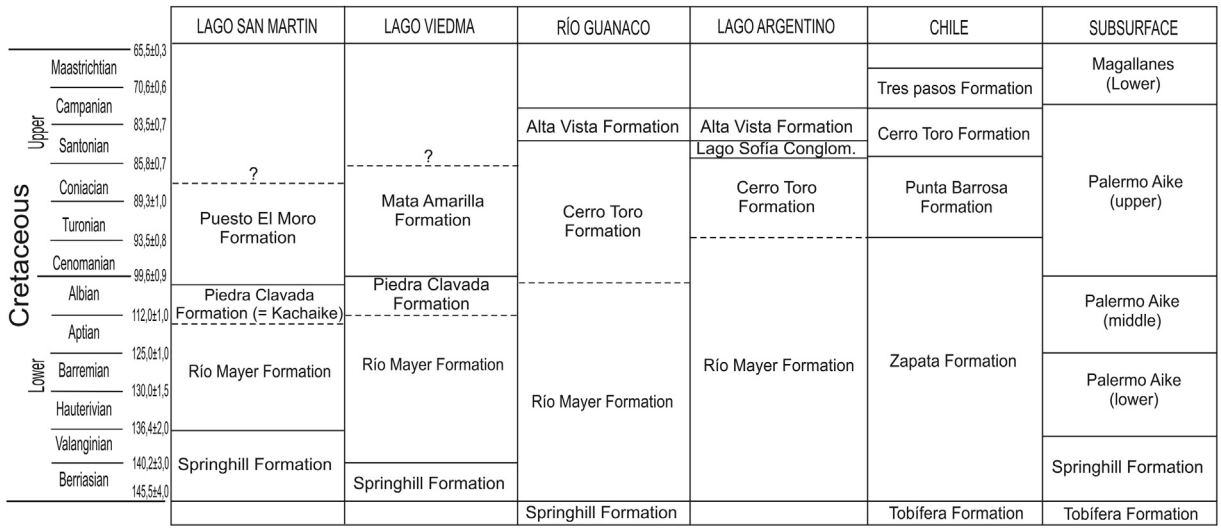

Fig. 2. Stratigraphic chart. Cretaceous of the Austral Basin (Argentina) in the study area, their comparison with the Rocas Verdes + Magallanes Basin from Chile and the subsurface names. Modified from Riccardi, 1971; Arbe, 2002; Fildani et al., 2003; Fildani and Hessler, 2005; Rodríguez and Miller, 2005; Varela et al., 2012; Richiano et al., 2012.

sandstones and less frequent conglomerates. The sandstones levels are generally between 0.05 and 0.5 m of thickness, massive or laminated, and occasionally with ripple cross-lamination (Richiano et al., 2012). This section presents similar body and trace fossil content that the previous sections described. In the last meters of the outcrops of this section were recorded *Chondrites*, *Ophiomorpha*, *Palaeophycus*, and *Zoophycos* associated with transported wood fragments containing *Teredolites* (Richiano et al., 2013; Richiano, 2015). The frequent intercalation of sandstone in the uppermost part of the unit is related to the distal influence of a deltaic system recorded in the Piedra Clavada Formation (Richiano et al., 2012). Two fossiliferous levels were described from the top of this section showing an age of Albian–Cenomanian times (Kraemer and Riccardi, 1997; Arbe and Hechem, 1984). TOC values from this section ranging between 0.67 and 1.81% in the beginning and very poor values towards the top (Richiano, 2014).

By contrast, the Río Mayer Formation at Lago San Martín locality (Fig. 1) is divided in two informal sections. The lower section is composed of laminated black shales and marlstones developed in outer shelf palaeoenvironments, associated with high abundance of ammonites of Hauterivian–Barremian age (Riccardi, 1971; Richiano, 2012). The upper section of the unit in the study area is characterized by the fine-grained aptian prodeltaic deposits, marking the transition to the Piedra Clavada (delta front) deltaic system (Fig. 3; Richiano et al., 2012). No TOC measurements where obtain from this locality.

In the subsurface the Río Mayer Formation corresponds to the Lower and (partially) Middle Palermo Aike members (Valanginian to Aptian), where the main source rock of Austral Basin is located. An average thickness of this interval is 250 m deposited over an approximate 20 My and it is composed by calcareous mudstones (Belotti et al., 2013). According to these authors, the beginning of the oil window start at about 2100 m depth in the transition between the forebulge and the foredeep of the basin (10,000 sq km), wet gas window is reached at 3500 m (5000 sq km), and dry gas window at 4300 m, basinward to the west (10,500 sq km), both in the foredeep basin (Belotti et al., 2013). Lower and Middle members of the Palermo Aike Formation have TOC values between 0.5 and 3; while kerogen types ranging from II, II/III to III (Belotti et al., 2013).

3. Sampling and methods

3.1. Fine-grained sediments

For this study we use the terms mudstone for siliciclastic (less than 15% of calcite) muddy sedimentary rocks without structure and shale for fissile/laminated rocks (Lundegard and Samuels, 1980; Potter et al., 2005). Limestones are considered as sedimentary rocks with more than 80% of calcite. On the other hand, for mix-composed rocks which are constituted by siliclastic material (quartz, feldspars, clays, etc.) and calcite components (bioclasts, micrite, calcite cements, etc.) we propose the terms marly-mudstone (between 15 and 30% of calcite), marlstone (30–70% of calcite) and marly-limestone (70–80% of calcite), in which abundances are taken from XRD results.

A total of 117 fine-grained rock samples from Río Mayer Formation were collected and analysed by XRD from three sedimentary sections in the Río Guanaco region (103 samples) and three sections at Lago San Martín (14 samples). Sampling was concentrated in the Río Guanaco region due to the better quality and more complete outcrops. Few samples from Springhill and Piedra Clavada Formations were also analysed by XRD in order to establish a comparative compositional analysis between the different units. Samples for XRD analysis were subjected to soft grinding with a rubber mortar, and repeatedly washed in distilled water until deflocculation occurred. The <2 μm fraction was separated by gravity settling in suspension, and oriented mounts were prepared on glass slides. Clay mineralogy was determined from diffraction patterns obtained using samples that were air-dried, ethylene glycol-solvated and heated to 550 °C for 2 h (Brown and Brindley,

Fig. 1. Location of the Austral Basin in South America and position of the sedimentary logs in the study area. A. Location of the Austral Basin in Patagonia, Argentina, and its thickness in subsurface (modified from Zanella et al., 2013). B. Thermal maturity of the subsurface of the Austral Basin (modified from Zanella et al., 2013). C. Study areas in Santa Cruz Province. D. Detail geologic map of the Lago San Martín locality and the sedimentary logs position. E. Distribution of outcrops located at Bahía de La Lancha, Lago San Martín locality. F. Detail geologic map of the Seccional Río Guanaco locality at Los Glaciares National Park and position of the sedimentary logs. Modified from Richiano et al., 2012.

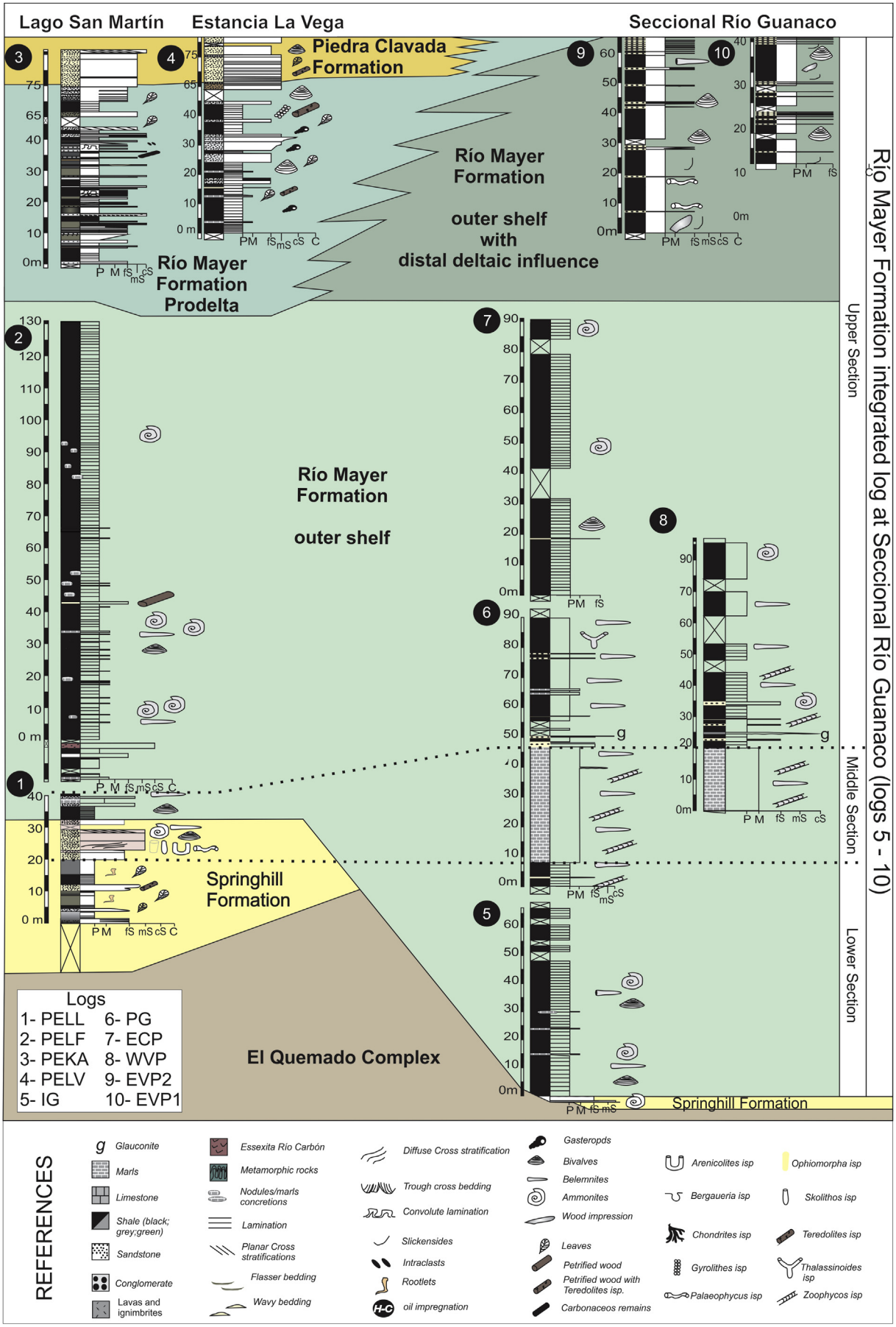

Fig. 3. Sedimentary logs from the Río Mayer Formation. References: P: pelite; M: marlstone; fS: fine-grained sandstone; mS: medium-grained sandstone; cS: coarse-grained sandstone; C: conglomerate. Log names as in Fig. 1.

Table 1
Results of X-ray diffraction for the lower section of the Río Mayer Formation at Seccional Río Guanaco locality. Samples names are linked to stratigraphic section names shown in Fig. 1F. Py: pyrite; I: illite; IS: illite-smectite mixed layer; Cl: chlorite; K: kaolinite; S: smectite; CMA: Clay mineral association.

	Whole rock							Clay fraction				
sample	Quartz	Feldspar	Calcite	Py	Clay	Association		I	IS	Cl	K	Clay mineral association
IG 1	11	2	78	1	8	ASSOCIATION A1	ASSOCIATION A	64	24	6	6	CMA I_a
IG 2	23	5	69	0	3			77	18	3	2	
IG 3	23	1	67	0	9			37	29	29	4	
IG 4	90	0	0	0	10			60	19	21	0	
IG 5	79	0	0	1	20			46	33	21	0	
IG 6	78	0	0	3	19			57	28	15	0	
IG 7	73	0	8	2	17			46	32	15	7	
IG 8	70	0	10	2	18			59	26	15	0	
IG 9	72	0	9	2	17			48	39	13	0	
IG 10 - 11	77	1	6	1	15			64	23	11	3	
IG 12 - 13	73	1	6	2	18			47	28	25	0	
IG14 - 15	80	1	0	2	17			46	36	16	2	
IG 16	19	0	78	0	3			38	30	21	11	
IG 17	52	1	32	1	14			34	42	20	4	CMA IS_a
IG 18 - 19	75	1	5	2	17			50	32	17	2	CMA I_a
IG 20 - 21	77	1	5	1	16			31	42	24	4	CMA IS_a
IG 22	80	3	0	0	17			41	37	20	2	CMA I_a
IG 23	79	1	4	0	16			42	30	25	3	
IG -24-25	78	2	6	0	14			29	40	21	10	CMA IS_a
IG 26	81	1	0	0	18			44	37	15	4	CMA I_a
IG 27 - 28	78	2	4	0	16			40	39	17	4	
IG 29	9	1	87	0	3			52	31	12	6	
IG 30 - 31	79	2	7	0	12	ASSOCIATION A2		35	44	18	3	CMA Is_a
IG 32 - 33	83	3	1	0	13			36	43	21	0	
IG 34 - 35	73	3	10	1	13			36	51	13	0	
IG 36	81	3	0	1	15			45	39	13	4	CMA I_a
IG 37 - 38	63	3	21	1	12			46	37	16	0	
IG 39	77	1	0	0	22			38	50	9	3	CMA Is_a
IG 40	72	0	15	1	12			34	44	15	7	
IG 41	35	0	53	3	9			48	34	12	6	CMA I_a
IG 42	85	2	2	0	11			41	35	20	4	
IG 43	76	3	6	0	15			34	40	20	6	
IG 44	79	3	0	1	17			37	40	20	3	
BP 1	71	2	18	2	7			41	27	23	9	
BP 2	67	5	14	1	13			26	29	41	4	CMA Cl_a
BP 3	34	25	20	1	20			6	17	76	0	
BP 4	74	3	9	1	13			40	32	28	0	CMA I_a
BP 5	71	2	15	1	11			55	27	16	2	

1980). Diffractograms were run on an X PANanlytical model X'Pert PRO diffractometer (CIG), using Cu/Ni radiation and generation settings of 40 kV and 40 mA.

For the whole-rock analysis semi-quantification was obtained from the intensity of the main peak for each mineral (Schultz, 1964; modified with own patterns; Moore and Reynolds, 1997). The estimation of the mineralogical components has a methodologically error ca. 10%. Crystallinity of clay minerals was deduced from the shape and sharpness of the XRD peaks (Brown and Brindley, 1980). Semi-quantitative estimations of the relative concentrations of the clay minerals were based on the peak area method following the methodology from Biscaye (1965). The response of the mineral species to sedimentation depends on the form of the particles (Pierce and Siegel, 1969); for that reason each mineral proportion is not directly proportional to the areas defined. Relative percentages of each clay mineral were determined by applying empirical factors (Moore and Reynolds, 1997). The abundance of different clay minerals in the <2 μm fraction is summarized in Tables 1–4.

Samples with illite and mixed-layer illite-smectite the Kubler index (KI) was measured from air-dried samples (Kubler, 1966). KI values were calibrated to the Crystallinity Index Standard (CIS) scale using the procedure and standards of Warr and Rice (1994). However the scarcity of this clay mineral in samples analysed here does not allow making a detailed analysis on it. The identified IS mixed layers, following the criteria of Moore and Reynolds (1997), were R0 (>50% smectite expandable layers) with (001) reflection near 14–15 Å in air-dried samples and 17 Å in ethylene-glycol solvated specimens, and R1 (40–20% smectite expandable layers) with reflections near 12–14 Å in ethylene-glycol solvated specimens. The relative abundance of illite and smectite in the IS mixed layers was determined by means of the $\Delta^{\circ}2\theta$ parameter (Moore and

Table 2
Results of X-ray diffraction for the middle section of the Río Mayer Formation at Seccional Río Guanaco locality. Samples names are linked to stratigraphic section names shown in Fig. 1F. References as in Table 1.

	Whole rock						Clay fraction				
sample	Quartz	Feldspar	Calcite	Py	Clay	Assoc.	I	IS	Cl	K	Clay mineral association
PG 1	62	2	30	0	6		39	37	18	5	CMA I_a
PG 2	70	5	18	0	7		60	21	17	2	
PG 3	68	2	23	0	7		26	40	34	0	CMA IS_a
PG 4	65	3	26	0	6		59	26	11	3	
PG 5	53	4	38	0	5		71	19	11	0	
PG 6	65	4	24	1	6		50	26	18	6	
PG 7	57	1	37	0	5		37	34	19	10	CMA I_a
PG 8	66	2	26	0	6		62	23	15	0	
PG 9	51	5	38	0	6		51	29	10	10	
PG 10	65	6	21	0	8		52	27	21	0	
PG 11	61	4	27	1	7		72	13	13	2	
PG 12	63	2	29	0	6		33	40	28	0	CMA IS_a
PG 13	60	6	28	0	6		61	26	10	4	
PG 14	55	2	37	0	6		69	13	14	4	
PG 15	39	5	49	1	6		61	20	11	8	CMA I_a
PG 16	71	4	17	0	8		64	23	13	0	
PG 17	50	2	40	0	8		85	12	3	1	
PG 18	62	2	34	0	2		43	47	9	1	CMA IS_a
PG 19	42	3	50	0	5		68	20	11	0	
PG 20	64	2	28	0	6		57	27	16	0	CMA I_a
PG 21	68	3	24	0	5		59	24	17	0	
PG 22	69	3	22	1	5		65	15	20	0	
PG 23	74	2	18	0	6		27	25	48	0	CMA CL_a
PG 24	58	5	26	1	10		66	18	16	0	CMA I_a
PG 25	69	1	25	0	5						
PG 26	67	2	26	0	5		33	30	36	0	CMA CL_a
PG 27	65	4	23	0	8						
PG 28	60	2	34	0	4		36	27	35	2	CMA CL_a
PG 29	53	4	37	0	6		61	17	23	0	CMA I_a
PG 30	30	2	63	0	5		20	37	43	0	
PG 31	69	2	22	0	7		41	22	37	0	
PG 32	60	13	21	0	6		22	27	51	0	CMA Cl_a
PG 34	83	5	2	0	10		29	6	65	0	
PG 35	74	10	7	1	8		38	23	39	0	
PG 36	79	7	4	0	10		37	12	51	0	
PG 37	61	17	0	0	22		71	0	29	0	CMA I_a
PG 38	77	9	0	0	14		22	0	78	0	CMA Cl_a

ASSOCIATION B

ASSOC. C

Reynolds, 1997). The empirical measure of the crystallinity of smectite was estimated from the measurement of the height of the (001) peak above the background (P) and the depth of the valley (V) on the low angle side on the glycolated sample, and then calculating the V/P in samples with higher smectite contents. A theoretical perfectly crystallized montmorillonite would have a V/P ~1 and poorer crystallinities would be represented by V/P values between 0 and 1 (Biscaye, 1965).

Conventional petrography was conducted in mudstones (3 samples), shales (6 samples) and marlstones (4 samples) in order to determine authigenic and diagenetic components of each type of lithology.

On the other hand, unprocessed chips of selected mudrocks (higher clay contents) were analysed by SEM in order to study the mineralogical micromorphology of clay and non-clay minerals. Samples were air-dried to constant weight before testing and coated with Au. Each sample was studied at several magnifications (12000, 15000 and up to 25000× in some cases) for optimal determination of both major and minor mineralogical components in order to show the microstructure details. Samples was analysed with a FEI Quanta 200 SEM and an EDAX Phoenix 40 (accelerating voltage 20 Kw, spot size from 3 to 4 μm, Facultad de Ingeniería, La Plata, Argentina).

Finally, for brittle analyses the following brittleness-indexes were applied:

BI Jarvie et al (2007): Qz/Qz + Ca + Cly, and,
BI Wang and Gale (2009): Qz + Dol/Qz + Dol + Ca + Cly + TOC

Table 3
Results of X-ray diffraction for the upper section of the Río Mayer Formation at Seccional Río Guanaco locality. Samples names are linked to stratigraphic section names shown in Fig. 1F. References as in Table 1.

	Whole rock						Clay fraction				
sample	Quartz	Feldspar	Calcite	Py	Clay	Assoc	I	IS	Cl	K	Clay mineral association
PG 39	26	44	6	0	24		85	0	15	0	CMA I_a
PG 40	75	7	2	0	16	A	61	11	28	0	
PG 41	37	40	5	0	18	S	66	2	32	0	
PG 42	84	3	7	0	6	S	22	21	57	0	CMA Cl_a
PG 43	14	43	34	0	9	O	56	0	44	0	CMA I_a
PG 44	25	15	46	0	14	C	20	20	60	0	
PG 45	84	8	1	1	6	I	34	13	52	0	
PG 48	79	2	10	3	6	A	25	24	51	0	CMA Cl_a
PG 50	66	3	23	2	6	T	24	40	36	0	
PG 51	75	4	11	2	8	I	22	34	44	0	
PG 52	75	2	5	6	12	O	26	34	40	0	
PG 54	73	12	4	2	9	N	45	14	41	0	CMA I_a
PG 55	70	14	5	2	9		39	23	38	0	CMA Cl_a
PG 59	84	7	0	2	7		41	31	27	0	CMA I_a
PG 60	65	7	16	3	9	C	34	21	45	0	
PG 64	67	10	13	3	7		41	24	35	0	
PEVP1-1	76	13	1	0	10		30	24	46	0	
PEVP1-2	69	16	0	0	15	A	32	9	58	0	
PEVP1-3	67	18	1	0	14	S	36	5	59	0	
PEVP1-5	64	24	0	0	12	S	30	19	51	0	
PEVP1-6	78	10	5	0	7	O	29	30	41	0	
PEVP1-8	76	11	4	0	9	C	28	20	51	0	CMA Cl_a
PEVP1-9	68	15	8	0	9	I	38	14	48	0	
PEVP1-10	72	14	7	0	7	A	28	21	51	0	
PEVP1-11	69	14	6	0	11	T	30	15	55	0	
PEVP1-13	74	15	3	0	8	I	39	11	49	0	
PEVP1-14	74	12	6	0	8	O	35	16	49	0	
PEVP1-15	78	14	1	0	7	N	32	19	49	0	
						D					

Where, Qz is quartz content, Ca is calcite, Cly is total clay content, Dol is dolomite (all measures from XRD) and TOC is total organic carbon. These formulas were applied to the samples where TOC values were obtained. For graphic purpose only the Wang and Gale index was showed because dolomite is inexistent or just a trace component (less than 1%) in the XRD data from Río Mayer Formation.

3.2. Sandstones

Considering that sandstones of Río Mayer Formation represent no more than the 5% of the outcrops, petrographic analyses were limited to a few samples (Richiano, 2012; Richiano et al., 2012). Conventional petrographic thin-sections (30 μm of thickness) were applied for textural and compositional analysis over 13 sandstones samples from Seccional Río Guanaco locality and four from Lago San Martín locality. Additionally, five sandstones samples of Springhill Formation and three from Piedra Clavada Formation were also analysed. These analyses were made using a polarization microscope Nikon Eclipse E-200 of the Centro de Investigaciones Geológicas, La Plata, Argentina (CIG). A detailed description of both detrital and authigenic components was carried out for each thin-section. Detrital components were used to classify the sandstones (according to Folk et al., 1970). Monocrystalline clasts were differentiated considering standard criteria of distinction (extinction, interference colour, cleavage, type of twinned, zonation, etc.) and rock fragments were distinguished. Modal composition was determined on a total of 13 thin-sections of sandstones and greywackes from Springhill, Río Mayer and Piedra Clavada formations (Table 5). The clast-counting in each thin section was made following Gazzi-Dickinson's methodology (Ingersoll et al., 1984) in which 400 points were assessed using a Swift points counter. When rock fragments have monomineral crystals bigger than 0.062 mm, they were considered as crystal clasts (method of Gazzi-Dickinson, Ingersoll et al., 1984). Samples with grain sizes greater or less were discarded for compositional classification although they were considered for the initial description of the detrital components. Considering that glauconite grains are sedimentary lithic fragments, in PG44, PELL11 and WVP11 samples of glauconitic sandstone facies, they do not be taken into account for the discrimination of source areas (Amorosi, 1995, 1997).

4. Compositional studies in fine grained-sediments

4.1. X-ray diffraction

4.1.1. Seccional Río Guanaco locality

Lower section (28 shales, 3 marly-shales, 4 marlstones, 2 marly-

Table 4
Results of X-ray diffraction for the Springhill, Río Mayer and Piedra Clavada formations at Lago San Martín locality. Samples names are linked to stratigraphic section names shown in Fig. 1D. References as in Table 1.

	Whole rock					Clay fraction					
sample	Quartz	Feldspar	Calcite	Py	Clay	I	Sm	IS	Cl	K	Clay mineral association
PSCH 4	71	0	0	0	29	5	0	4	0	91	
PEF 4	56	16	5	1	22	11	0	56	33	0	CMA Cl_a
PEF 5	4	5	88	1	2	0	0	0	0	0	
PEF 10	45	15	17	5	18	6	0	45	49	0	
PEF 11	5	22	67	3	3	18	0	22	60	0	
PEF 12	74	6	7	1	12	9	0	50	41	0	
PEF 15	64	12	3	2	19	15	0	32	53	0	
PEF 17	55	4	31	1	9	17	0	39	44	0	
PEF 20	16	40	6	12	26	0	0	16	84	0	
PEF 21	48	8	33	2	9	19	0	28	53	0	
PEKA 1	57	4	0	2	37	0	99	0	0	1	CMA S_a
PEKA 11	62	11	2	1	24	0	94	0	0	6	
PEKA 14	76	4	2	0	18	0	96	0	0	4	
PEKA 17	64	12	5	2	17	0	98	0	0	2	

Table 5
Detritic modes of sandstones from the Springhill (FSp), Río Mayer (FRM) and Piedra Clavada (FPC) formations.

Region	Unite	sample	Qm	Qp	F	LV	LG	Matrix	Palaeoenvironment
Río Guanaco Locality	F. Sp	WVP2	62.28	3.51	12.28	21.93	0.00	68.75	inner shelf
		WVP3	74.22	1.74	1.74	22.30	0.00	28.25	
	F. R M	BP3	90.61	3.87	4.42	1.10	0.00	28.75	outer shelf
		PG39	69.53	3.00	18.88	8.58	0.00	7.25	
		PG44	12.85	1.12	7.82	3.35	74.86	30.25	
		WVP11	24.57	0.00	9.00	2.08	64.36	27.50	
		PEVP1 7	4.81	1.92	91.83	1.44	0.00	33.25	outer shelf with deltaic influence
Lago San Martín Locality	F. Sp	PELL7	78.14	21.86	0.00	0.00	0.00	0.00	inner shelf
		PELL8	73.47	12.24	0.00	14.29	0.00	56.25	
	F. R M	PELL11	17.87	6.76	8.21	4.83	62.32	47.00	
		PEKA20	39.01	34.98	12.11	13.90	0.00	25.00	prodelta
	F. PC	PEKA22	25.32	12.03	16.46	46.20	0.00	43.00	delta front
		LV29	15.82	8.54	4.43	71.20	0.00	14.50	

limestones and 1 limestone samples; Table 1). Whole-rock compositional data shows that quartz is the prevalent mineral (between 9 and 90%; 65.7% in average); followed by calcite in varied abundance (0–87%; 22.9% in average), while clay (3–22%; 13.6% in average) and feldspar (0–25%; 2.9% in average) are less frequents (Fig. 4). Clay-fraction (<2 μm), XRD analysis show that this section is characterized by illite, chlorite and mixed-layer illite-smectite (IS) in relatively similar abundances (Table 1), with a slight dominance of illite over the other two is observed. Although kaolinite is almost absent, it occasionally can appear in lower concentrations (<5%) (Fig. 4).

Middle section (5 shales, 21 marly-shales and 10 marlstone samples; Table 2). Whole-rock compositional data of this section is characterized by calcite occurrence (20–30%) however quartz is still the main component (62% in average). In the last 5 m of the section clays and feldspars increase while calcite decreases (samples PG34 to PG38) (Fig. 4). In clay-fraction illite prevalence is observed (50%) accompanied by lower contents of chlorite (25%) and IS (23%) (Fig. 4).

Upper section (24 mudstones, 2 marly-mudstones and 2 marlstone samples; Table 3). In this section the whole-rock data indicates the prevalence of quartz (between 14 and 84%, average 66.6%), accompanied by feldspar (2–44%, 14% in average) and clays (6–24%, 10% in average). Calcite is less frequent than in the other studied sections (9% in average ranging from 0 to exceptionally 46%). In clay-fraction chlorite (43% in average) predominates over illite (39% in average) and IS (18% in average) (Fig. 4).

4.1.2. Bahía de la Lancha in lago San Martín locality (Fig. 5; Table 4)

Whole-rock analysis shows that a sample of a siliciclastic mudstone obtained from flood plain of Springhill Formation has abundant quartz proportions (71%) and moderate clays (29%) (Fig. 5). The marine facies of the Río Mayer Formation can be subdivided into two different compositional segments. The lower part of the succession (samples PEF 4 to PEF 11) presents calcite concentrations ranging from 5 to 88% (average 44%), the quartz content is very variable between 4 and 56% (average 27.5%), feldspars and clays are present in similar proportion (14% and 11% in average

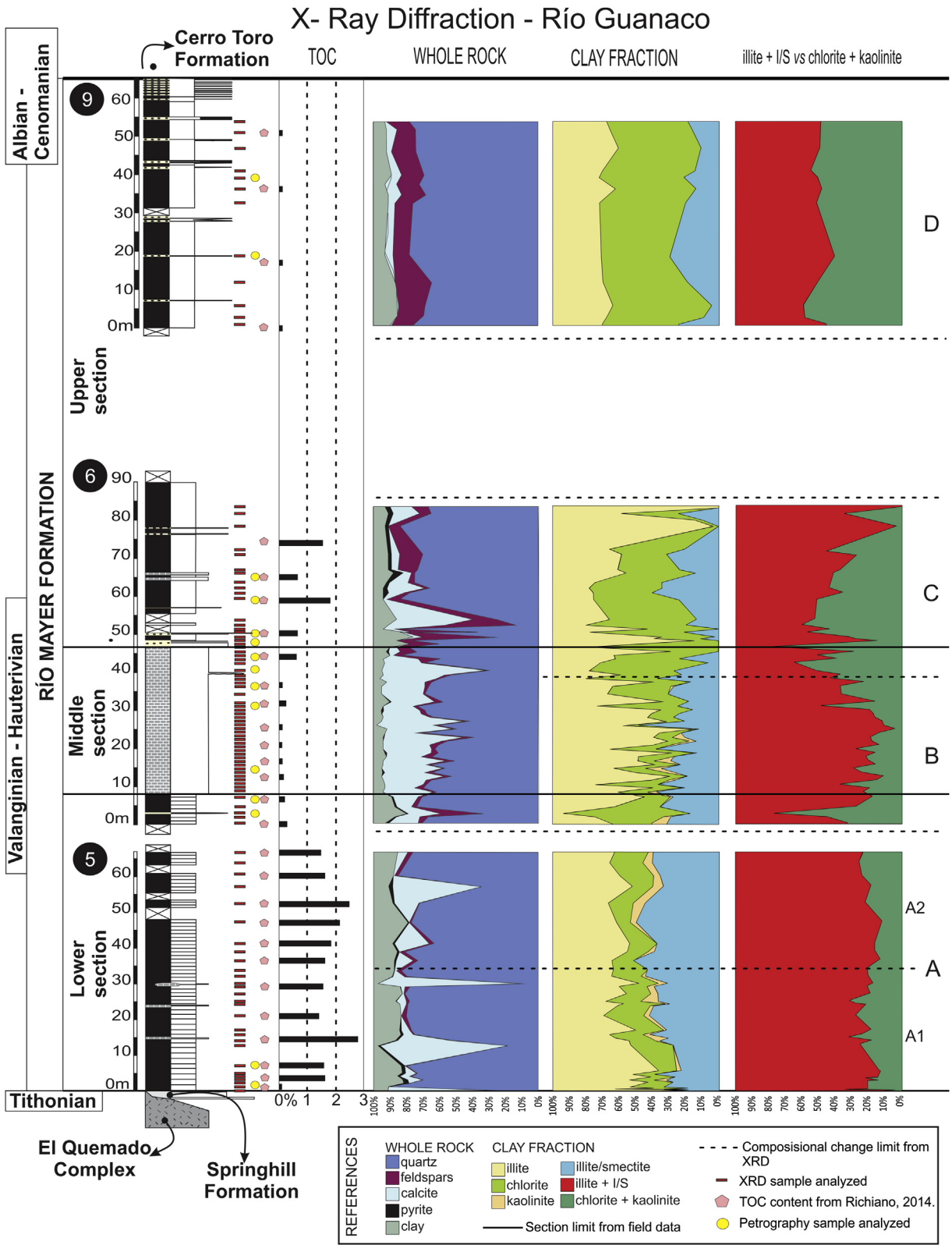

Fig. 4. X-ray diffraction. Results of the Seccional Río Guanaco locality and the main mineralogical associations recognized (A–D). TOC values from Richiano, 2014.

respectively) (Table 4, Fig. 5). On the other hand, the upper segment (samples PEF 12 to PEF 21) is dominated by quartz (16–74%, 51.4% in average), while calcite proportions are generally moderate (3–33%, 16% in average) (Fig. 5). Feldspar is present between 4 and 40% (average 14%) and clay minerals vary generally from 9 to 26% (15% in average). Samples from the prodelta deposits of the Río Mayer Formation are mainly composed by quartz (57–76%, 64.75% in average) with less feldspar (7.75% in average) and clay

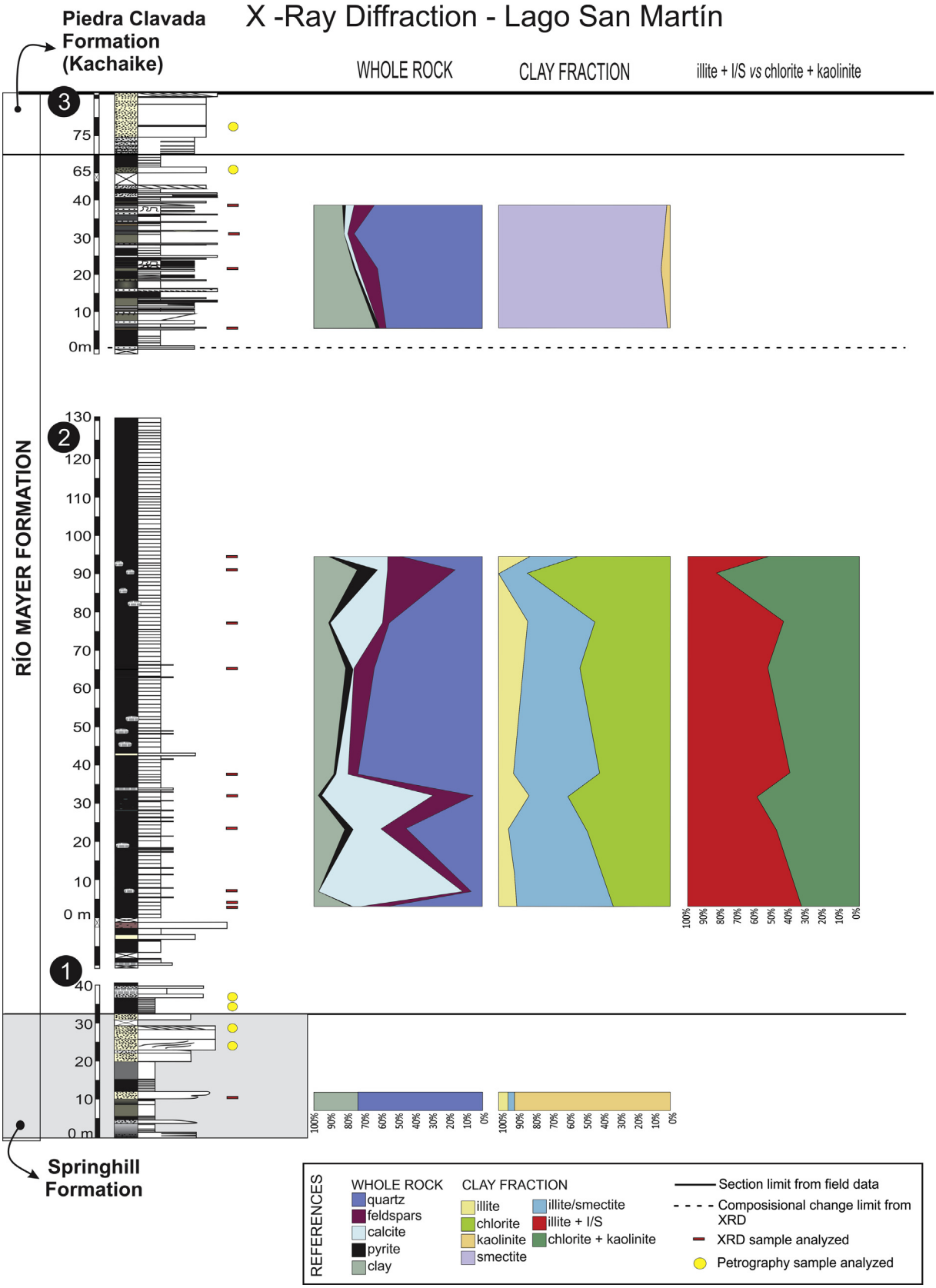

Fig. 5. X-ray diffraction. Results of the Lago San Martín locality.

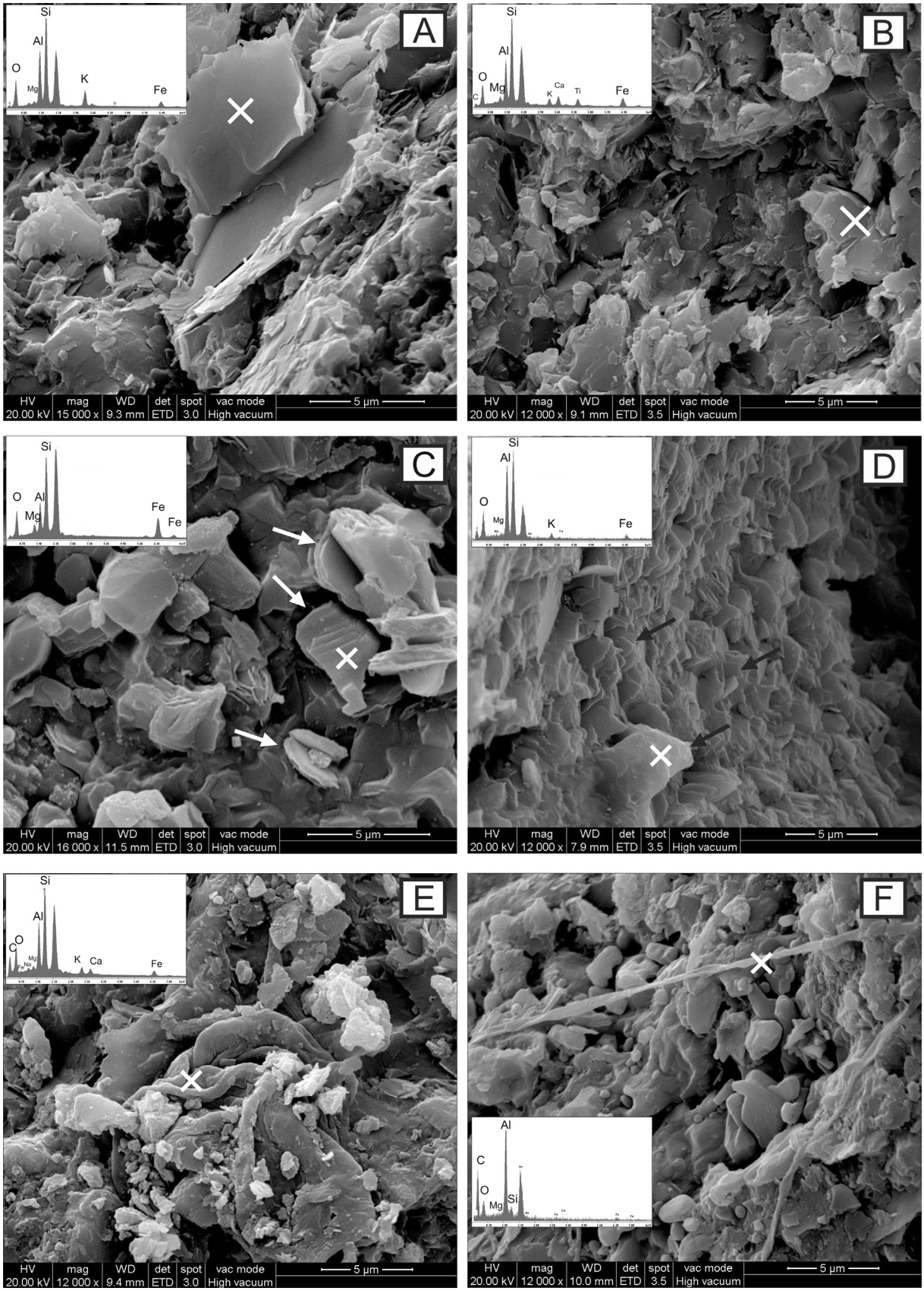

Fig. 6. SEM microphotographs and EDAX results. A, B. illites, photos show high fragmented clays of illite with variable size, irregular borders and without a preferential order. C. Authigenic chlorites appear as stacked sheets with border dissolution (white arrows). D. IS mixed layers ordered regarding 001 plane (black arrows). E. branched organic matter intergrown with detrital and removed clays. F. elongated biofilms of organic composition over a clay-micrite mixture (marlstone). The cross indicates the point measured by EDAX analysis of mayor elements.

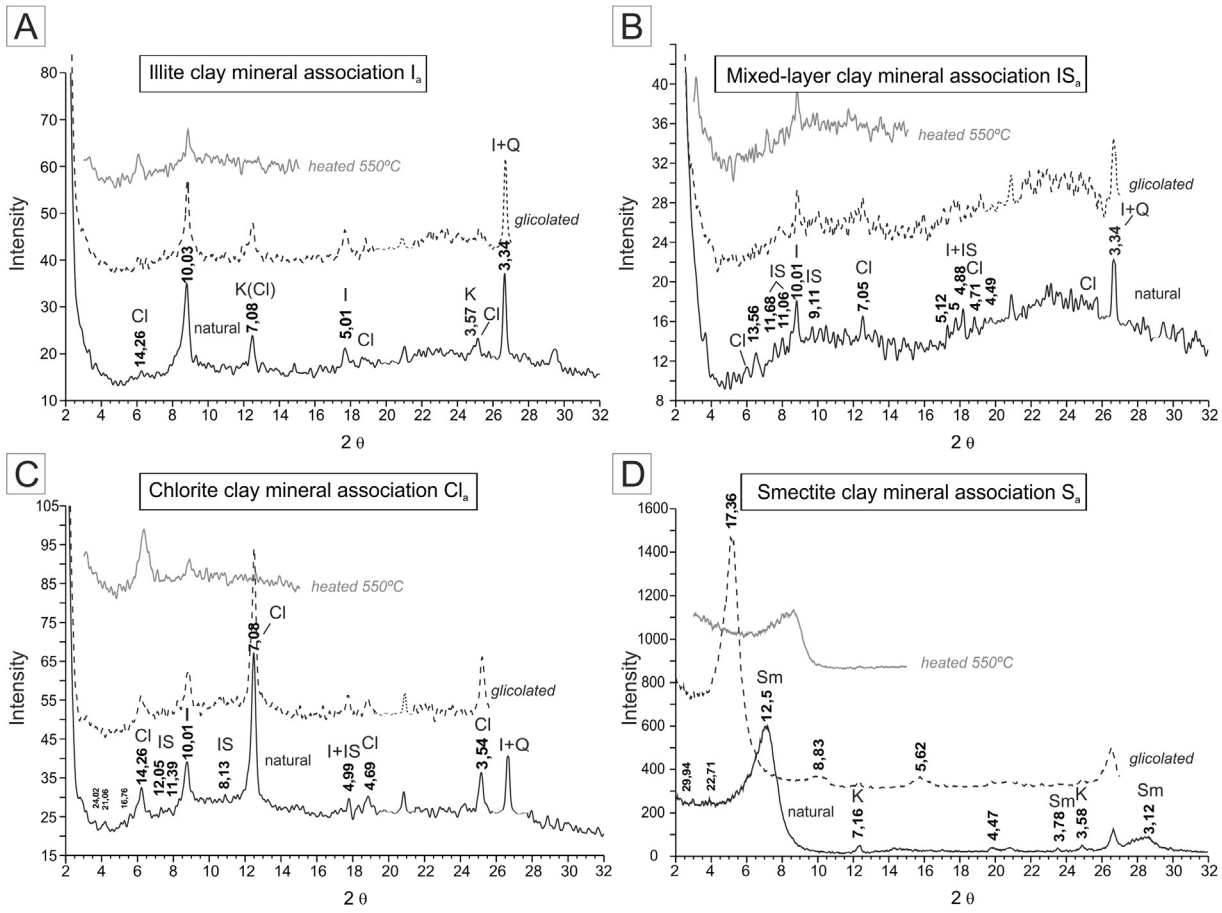

Fig. 7. X-ray diffractograms of the clay assemblages from Río Mayer Formation. A. Illite assemblage (I_a). B. IS mixed layer assemblage (IS_a). C. Chlorite assemblage (Cl_a). D. Smectite assemblage (S_a).

proportions (24% in average); calcite is almost absent (0–5%) (Fig. 5).

Clay-fraction shows a strong difference between the clay mineral compositions of the three formations. In Springhill Formation kaolinite is clearly dominant (91%), with illite and IS in scarce contents (Fig. 5). On the other hand, chlorite prevalence (46% in average) in Río Mayer Formations outer shelf sediments is associated with IS mixed-layers (32%) and illite in less proportion (11%) (Fig. 5). Finally in the fine sediments form the prodelta (transition to Piedra Clavada Formation) smectite is the predominant (97% in average) accompanied by scarce kaolinite (Fig. 5).

4.2. XRD and SEM characterization of clay minerals

XRD analysis allow to recognize the illite crystallinity (KI) which varies between 0.2 and 0.65 which make possible to suggest the presence of at least two different polytypes, the 1M with crystallinity indices >0.4 related to diagenetic origin and the $2M_1$ type with high crystallinity which is thought to have a metamorphic origin (Fig. 7A).

On the other hand, the position of main peaks of chlorite is in agreement with iron rich chlorite type, and polytypes observed are similar to those of low temperature during diagenesis.

The difference in 2°θ between peaks (002 and 003) of mixed-layer illite-smectite in glycolated samples vary from 7.8 to 5.6 which indicates that proportion in smectite is between 20 and 80% (Moore and Reynolds, 1997). Particularly in the Section 5 (IG) the smectite proportion in IS varies from 30 to 60%, in Section 6 (PG) from 40 to 70% and in Section 9 (EVP1) from 50 to 70%.

Smectite has well-defined reflections and V/P ratios ranging between 0.8 and 0.5. Variable basal reflection of smectite (between 12.4 and 14.7 Å) (Fig. 7D) suggests that interlayer occupancy is not uniform in the prodelta facies.

Clay mineral micromorphology recognized by SEM analyses shows that mostly of the clays are non-oriented, detrital, with irregular borders and with basal sections (001) lower than 5 μm (Fig. 6). EDAX analysis of clays of illitic composition (illite and IS; Fig. 6A, B) show a dominance of Si, Al and K with lower proportions of Fe, Mg and Na, and occasionally Ca and Ti. Chlorite is identified in crystals of 2 or 3 μm, in which the contents of Fe and Mg are much higher, where Fe the dominant (Fig. 6C).

Additionally, SEM analyses reveal that IS clays show thin flakes as the main micromorphology which are ordered according the 001 faces. Flakes show equidimentional subhedral forms with defined borders in crystals with less than 3 μm. EDAX shows Si and Al as the majority cations, followed by K, Mg and Fe, (Fig. 6D). These results are consistent with the XRD analysis.

Organic matter was also identified by SEM (Fig. 6E–F) and shows intergrown with illite and IS with characteristic morphologies of branched and twisted fibbers (Fig. 6E) or as elongated fibbers also known as biofilms (Fig. 6F). In both cases the EDAX analysis show peaks of C of high intensity accompanied by other peaks from the clays of the rock (Al, Si, K, etc.; Fig. 6E–F).

4.2.1. Clay mineral assemblages

In the Río Mayer Formation four clay mineral assemblages are

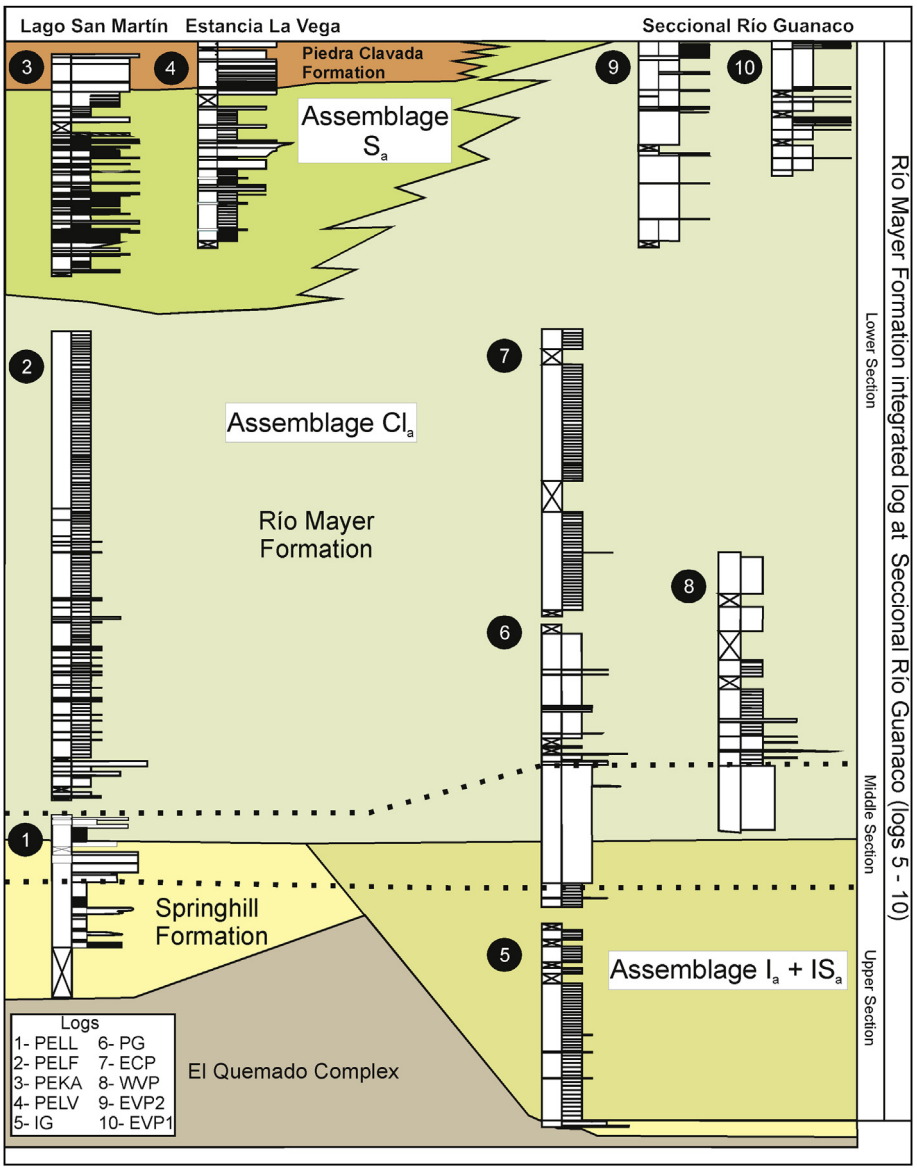

Fig. 8. Distribution of the clay mineral assemblages recognized in the studied sections.

characterized on the basis of the presence, type and relative amount of the clay minerals. These assemblages are present in all of the analysed sections (2, 3, 5, 6 and 9).

Illite-dominated assemblage (I_a; 51 samples; Fig. 7A): is characterized by presence of illite in more than 40%, varying from 40 to 85% and accompanied by illite-smectite mixed layers (11–39%) and in less proportion chlorite (3–29%) and kaolinite (0–11%).

Illite-smectite mixed layers assemblage (IS_a; Fig. 7B): is differentiated of I_a assemblage by the higher proportions of IS (>40%), recognized in 13 samples which also have illite (30–40%), chlorite (9–24%) and less common kaolinite (0–10%).

Chlorite dominated clay mineral assemblage (Cl_a; 35 samples; Fig. 7C) shows the higher contents of chlorite (>35%) which reach up to 84% accompanied by variable IS contents (6–50%), illite (6–41%), and kaolinite is almost absent with the exception of two samples with less than < 4%.

Smectite dominated assemblage (S_a; 4 samples; Fig. 7D): is characterized by high abundance of this clay mineral (Sm> 90%) and scarce kaolinite (1–6%).

4.2.2. Distribution of the clay mineral assemblages of Río Mayer formation

I_a and IS_a assemblages are closely associated and both are concentrated in the basal portion of the lower section of the Río Mayer Formation. IS_a occurs interlayered with I_a assemblage in a spaced way (Fig. 8, Tables 1 and 2).

Cl_a is concentrated in the upper 15 m of the middle section and widespread in all the upper section of the Río Mayer Formation in the Seccional Río Guanaco locality. Some interlayers with the I_a assemblage is also recognized, and also occurs in the section 2 of Lago San Martín locality (Fig. 8; Tables 2–4).

S_a is only identified in the Section 3 (Fig. 8; Table 4) which characterizes the prodelta facies which dominates in this section.

4.3. Petrography of shales, mudstones and marlstones

4.3.1. Shales

Shales are characterized by fine clay minerals (few microns) intergrown with undifferentiated material and organic matter in

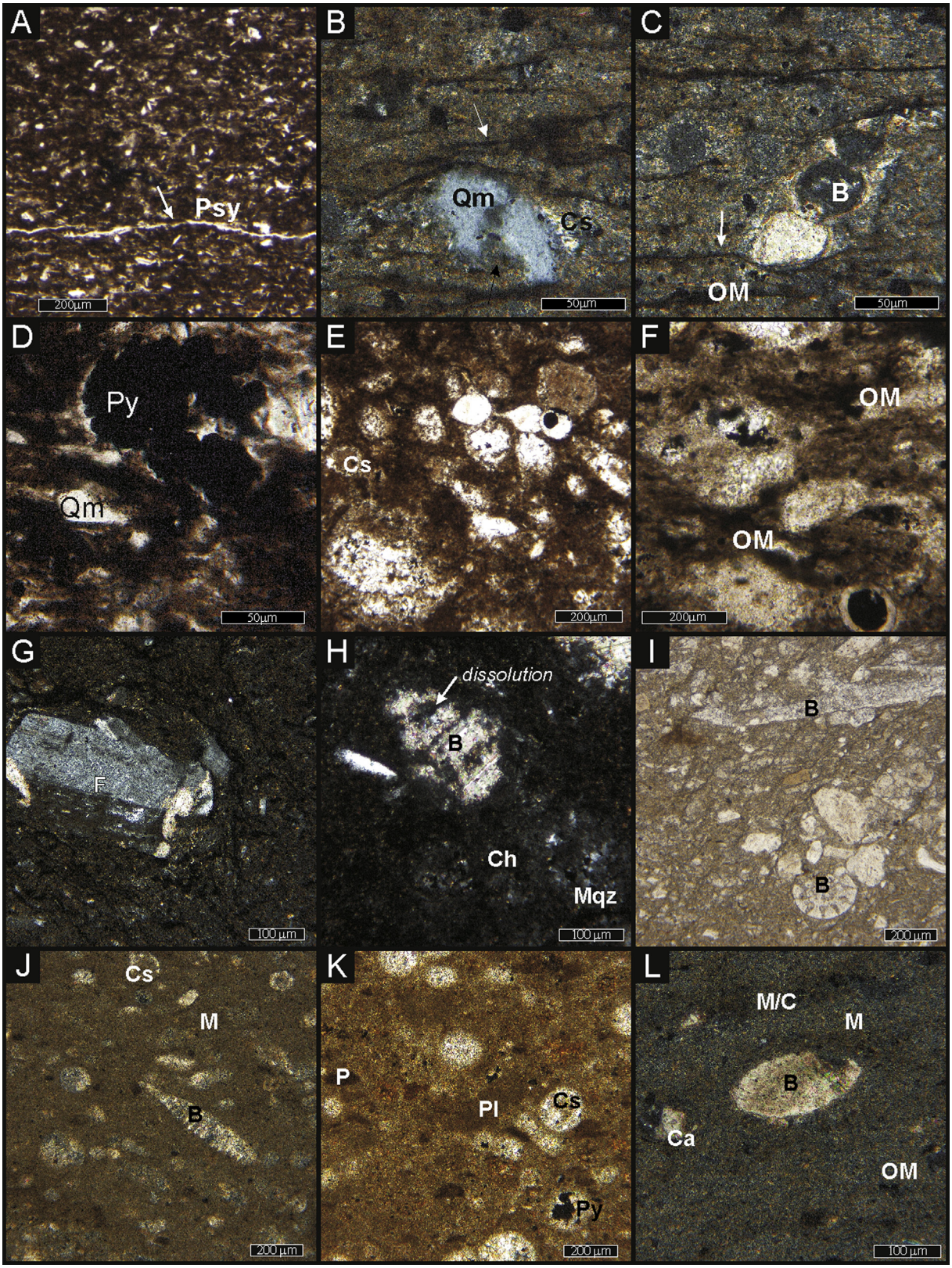

Fig. 9. Petrology of fine-grained sediments. A–D. Black shales. A: Shows detrital fine grains of quartz, feldspars, clays, opaques which are surrounded by undifferentiated material with high content of organic matter; a pseudostylolite is observed orientated according lamination. B: a detail of quartz grain with dissolution, calcite cement associated. C: Foraminifer fragmented with recrystallized walls in a base of fine grained mudstone with seams of organic matter. D: a detail of the shale with organic matter and framboidal pyrites grouped. In pictures A–C the white arrows show that lamination is commonly an interlayer between organic-rich and mineral-rich laminae. E–H. Mudstones. E: Bioclasts, clacispheres, and other calcite fragments without recognizable texture are surrounded by mudstone with some detrital micas. F: calcite fragments without recognizable texture, some sectors show organic matter concentrated and pyrite crystals. G: feldspar with carsbald twin partially altered to calcite. H: mudtone with a recrystallized bioclast. I-L. Marlstones. I: bioclastic marly-packestone with fragments of equinoderms and bivalves. J: marly wackestone with abundant calciespheres and bioclasts, the base is micritic mixed

variable proportions from scarce to moderate (Fig. 9A). Monocrystaline quartz grains are rare and show angular forms with corroded boundaries, usually of less than 60 μm (Fig. 9B), fragments of plagioclase (20–30 μm), which eventually preserve their polysynthetic twinning, are very scarce to sporadic and show commonly dissolution in crystal boundaries. The carbonate fragments are rare and consist of very fragmented bioclasts with poor recognizable micromorphology (Fig. 9C). Opaque minerals include pseudocubic crystals of pyrite which appear as aggregates or as individual crystals (Fig. 9D).

The most common cement is composed by chert filling microveins or as replacement of carbonate fragments, and also filling pore cavities. Argillic cements are scarce and usually appear surrounding quartz clasts (coatings; Fig. 9A). Lamination is commonly very penetrative and shows an interlayer between organic-rich and mineral-rich laminae (white arrows in Fig. 9B, C). Dissolution seams are common and show irregular layers with organic matter and undifferentiated fine material concentrated in these microstilolytes. Organic matter also occurs dispersed or filling irregular pores (Fig. 9A, D).

4.3.2. Mudstones

Muddy rocks are characterized by clay minerals of fine-to very fine-grained size with an irregular to ondulouse lamination where organic matter and undifferentiated fine material is concentrated (Fig. 9E, F). Opaque minerals are also abundant and diseminated in muddy rocks. Silt and sand clasts are very rare and composed by very fine angular monocrystalline quartzs of tens of microns (30 μm in average) with border dissolution. Feldpars are very scarse and occur with carsbald twin (orthoclase FK) which are commonly altered and replaced by calcite; some crystals show up to 600 μm (Fig. 9G). Pseudo-intraclasts (Flügel, 2004) (≤500 μm) are common showing rounded and diffuse borders. The carbonate fragments are scarce and some of them show non-recognizable skeletal morphologies, and with high replacement by siliceous cements in which chert and microquartz predominates (Fig. 9H). These silica cements are recognized mostly as patches. Incipient irregular lamination associated with dissolution surfaces is also observed.

4.3.3. Marly-mudstones, marlstone and marly-limestones

The components of these lithologies are divided into carbonate and terrigenous, the former are generally more abundant although they vary between 15 and 80%. The three lithologies consider grade between each other.

Carbonate fragments: are moderate to abundant and consist mostly of skeletal fragments (bivalves, gastropods, spicules, echinoderms, foraminifera and coccoliths, Fig. 9I–L) some of which are highly recrystallized and with partial replacements by siliceous cements. Non skeletal fragments consist mainly of calcispheres, pseudo-intraclasts and micritic peloids (Fig. 9J, K). Pseudo-intraclasts, as in the mudstones, appear associated to intense bioturbated levels.

Terrigenous: in order of abundance are constituted by very scarce potassic feldspar with subhedral to anhedral crystals, small and very angulous monocrystalline quartz and very scarce micritic pseudo-intraclasts (Fig. 9K).

Matrix: micrite is the most common component in the matrix (Fig. 9J–L), which can be mixed with clays (mostly detrital illite; Fig. 9L), opaques, organic matter and undifferentiated fine material. Some sections in the matrix show recrystallization of calcite to microsparite and sparite (Fig. 9L) and partial replacements by chert.

In some cases marlstones show bands of light and dark colourations with more carbonate or more organic matter content respectively. Cements are generally very scarce and constituted by calcite and chert. Calcite appears filling small pores or veins with anhedral crystals of sparite and macrosparite. Siliceous cements are very scarce and are recognized in pores, small cavities or as partial replacement of skeletal fragments and calcispheres (Fig. 9J, K). Recrystallization of calcite (by aggradation) is observed in some parts of the matrix associated to intermittent pseudostylolites (by pressure-dissolution during chemical compaction). Organic matter is also observed disseminated or forming an irregular mottled (Fig. 9J–L).

5. Sandstone petrography

The sandstones of Río Mayer Formation (N = 7; Table 5) are matrix supported with 31.7% in average of protomatrix. Samples are graywackes, except for one sample (PG39; Table 5) which is clast-supported. The grain size of detrital components varies between very fine-to fine-grained sand (62–250 μm), and exceptionally some grains are as coarse as 500 μm. Petrographic analysis allows to recognize that detrital mode is represented by nine main components, in order decreasing of abundance: monocrystalline quartz (Qm), polycristalline quartz (Qp), potassium feldespar (Fk), plagioclase (Pl), biotite (Bt), opaque grains (Op), volcanic lithics (Lv), bioclasts (B) and glauconite lithics.

5.1. Detrital components

Monocrystalline quartz (Qm): this component is the main component of The Río Mayer Formation in most cases being in proportions of up to 90%, with an average of 37%; although it can occasionally be very scarce (5% in the sample PEVP1-7). Crystals have straight extinction, commonly with embayments and occasionally with negative inclusions of volcanic glass associated with a volcanic origin. The grains are subrounded to subangular, and less commonly, subhedral clasts are present. In some cases, crystal clasts are elongated and show undulating extinction related to a metamorphic origin. The grain size of this component varies between 1000 and 200 μm (Fig. 10A, B).

Polycrystalline quartz (Qp): these grains are scarce to moderate, ranging between 0% and 20%, with an average of 4%. Grains are subangular to subrounded and range from 200 to 400 μm. Individual crystals are anhedral, elongate to ribbon-shaped, with undulating extinction and sutured boundaries (indicating a metamorphic origin, Fig. 10C, D). Sporadically, polycrystalline quartz shows equidimensional crystals with straight boundaries; the latter could have both a sedimentary or metamorphic origin.

Plagioclase (Pl): this component are very scarce to scarce, ranging from 0.2 (PELL11) to 16.7% (PA7), with an average of 4%. Grains are subhedral and subangular, and occasionally subrounded. The grain size is 200 μm on average. They are twinned according to the albite (Fig. 10E, F) and, less commonly, Carlsbad laws. The plagioclase composition determined by Michel-Levy method varies from oligoclase to andesine. They frequently show alteration to clay minerals which are concentrated both in twin planes and fractures.

Potassium feldspar (Fk): the potassium feldspars are more abundant than plagioclases; and are, following quartz, the most abundant component in sandstones. These crystals range from 0.2% (PG44) to 31% (PEVP1-7) (~9% on average). They are equidimensional and varies between 100 and 200 μm. Grains are twinned

with clays and very fine grained detrital minerals. K: marlstone with peloids, altered lithoclasts, pseudo-intraclasts, calciespheres and framboidal pyrite. L: marlstone constituted by micrite and clayminerals intergrouded with scarse bioclasts and calcite fragments. References: Qm: monocrystaline quartz; F: feldpar; Py: pyrite; B: bioclast; M: micrite; C: clay; P: peloid; PI: pseudo-intraclast; Cc: calcite cement (sparite); Cs: calcisphere; Ca: esparite; Ch: chert; Mqz: microquartz; Psy: pseudostylolite.

according to the Carlsbad law and occasionally show oscillatory zonation. Feldspars usually show different degrees of alteration (Fig. 10G, H).

Biotite (Bt): is present in very scarce proportions (<3%). The grains are green in colour, have perfect cleavage and pleochroism; and show high interference colors and parallel extinction in cross-polarized light (Fig. 10I, J, K). The crystals are angular to subangular with long prismatic shapes and vary between 50 and 300 μm in size. Biotite frequently shows different degrees of compaction strain deformation. Generally is concentrated in lamination planes, although eventually are scattered throughout the sandstone sample.

Opaque grains (Op): they are present in scarce proportion, ranging from 1 to 5 %. The grains are subrounded to rounded and frequently constitute speckles (Fig. 10L). Among these, a common component is pyrite crystals.

Other detrital components: this group includes the volcanic lithics (Lv), the bioclasts (B) and glauconitic lithics (Lg). The bioclasts are rare, and only fragments of shells are recorded in some sandstones of profile 1 (Fig. 11A, B; PELL). Volcanic lithics are rare (generally less than 4%) and are concentrated in prodelta deposits in the Lago San Martin and Estancia La Vega localities (Figs. 1 and 11C–J), where can reach up to 14%. The volcanic lithic clasts of the Río Mayer Formation are distinguished by their microtexture and/or composition in four different types: with pilotaxitic texture (Lvp), with spherulitic texture (Lve), with trachytic texture (Lvt) and rhyolitic lithics (Lvr).

The volcanic lithics with pilotaxitic texture (Lvp) are documented by the presence of small plagioclase crystals, euhedral to subhedral, immersed in an aphanitic groundmass (Fig. 11C, D). This pilotaxitic texture is characteristic of intermediate volcanic groundmass (Best and Christiansen, 2001).

The volcanic lithics with spherulitic texture (Lve) are subrounded with pale yellow to brown colours. They are characterized by the presence of recrystallized volcanic glass, which sometimes generates a typical spherulitic texture (Fig. 11E, F). Their origin could be pyroclastic, although there have been no glassy shards to confirm this hypothesis. Another source would be from recrystallization of volcanic aphanitic groundmass.

Volcanic lithics with trachytic texture (Lvt): these volcanic lithics are characterized by small crystals of plagioclase with their major axes oriented parallel, immersed in an aphanitic groundmass (Fig. 11G, H). This texture is typical of the intermediate to acid volcanic rocks, especially trachytes, though is also present in andesites and dacites (Best and Christiansen, 2001).

Finally volcanic rhyolitic lithic fragments (Lvr) consist of crystals of quartz and feldspar immersed in an aphanitic groundmass (Fig. 11I, J).

The four types of volcanic lithics are characterized by subrounded shapes and grain sizes ranging from fine to coarse-grained sandstone. They are concentrated in the samples of the region between the Viedma and San Martín lakes (Figs. 1 and 3) both in the upper section of the Río Mayer Formation as in Piedra Clavada Formation.

Glauconite lithics (Lg): this particular type of sedimentary lithic is present as abundant components at three levels of glauconitic sandstones (PG44, WVP11 and PELL11) with proportions varying between 62 and 75%. They are very well rounded to rounded with clay coatings; they are recognized by the typical greenish colour (Fig. 11K, L).

5.2. Cements

The predominant type of cement in the sandstones of the Río Mayer Formation is carbonate sparitic-type with a blocky distribution (Fig. 12A, B). It is composed of coarse mosaics of calcite with poikilotopic texture that completely closes the pore spaces. Occasionally dissolution of clasts can be observed by pervasive calcite cementation (Fig. 12C). In lower proportion some samples shows a subordinate ferruginous cement (iron oxides cement), which is shown surrounding the clasts as coating or as filling pores and patches (Fig. 12D). It has also been recognized clay cement associated with dissolution of clasts (Fig. 12E). On the other hand, quartz cement is the most common in sandstones of Springhill Formation. It shows the secondary growth in optical continuity with the quartz grains (Fig. 12F).

6. Sandstone classification

As shown in Fig. 13, the sandstones of the Río Mayer Formation are predominantly lithic and feldspathic graywackes (6 samples) and one sample corresponds to a subarkose arenite (Fig. 13A). Following compositional diagram of Folk et al. (1970), these samples are litharenites (4), sublitharenite (1), arkose (1) and lithic arkose (1) (Fig. 13B).

The sandstones of the Springhill Formation are two from the Seccional Río Guanaco and two from Lago San Martín localities, of which three are lithic graywackes and one is a sublithic arenite (Fig 13A). In the ternary diagram of Folk et al. (1970), these sandstones are classified as sublitharenites (2), feldspathic litharenite (1) and litharenite (1) (Fig. 13B).

The two samples of sandstones from the Piedra Clavada Formation at Lago San Martin and Estancia La Vega localities (Fig. 1) correspond to a lithic graywacke and lithic arenite (Fig. 13A). According to Folk et al. (1970), they are classified as litharenites (Fig. 13B).

7. Discussion

7.1. X-ray diffraction

In Seccional Río Guanaco locality, Río Mayer Formation rocks are almost entirely composed of variable proportion of quartz (9–90%), feldspar (0–44%), calcite (0–87%) and clays (3–24%). Clay minerals are mostly constituted by illite, chlorite and IS in order of abundances. Whole-rock mineral assemblages show the same composition with variable contents along the section (Fig. 4).

Assemblage A in whole-rock is characterized by quartz as the main component (65% in average), scarce feldspar (3%) and scarce clays (13.6%). Calcite is concentrated in certain levels in the lower part of this assemblage (A1), while in the upper part quartz is the main component (A2). In the clay-fraction (<4 μm) illite is the main component (43% in average) with IS (34% in average), both constitute near of 80% of the total clays, while the remaining 20% corresponds to chlorite (Fig. 4; Table 1).

Assemblage B in whole-rock is characterized by the occurrence of calcite (30% in average), the minor proportions of clays (6%), and quartz that remains abundant (60%). Clays recognized in clay-fraction are similar in type and proportion to the previous assemblages (Fig. 4; Table 2).

Assemblage C in whole-rock is characterized by quartz dominance (65% in average) with an increase in clays (11%) and feldspar (12.8%) while calcite decreases (11%), which refocuses in specific intervals (PG43, 44). In clay-fraction chlorite is the prevalent (40% in average) compared with previous assemblages (Fig. 4; Table 3).

Finally, D assemblage in whole-rock shows abundant quartz contents (72% in average) and increases in feldspar (15%). Clay percentages is constant (10%) and calcite decreases regarding previous assemblages (4%). In clay-fraction chlorite proportions

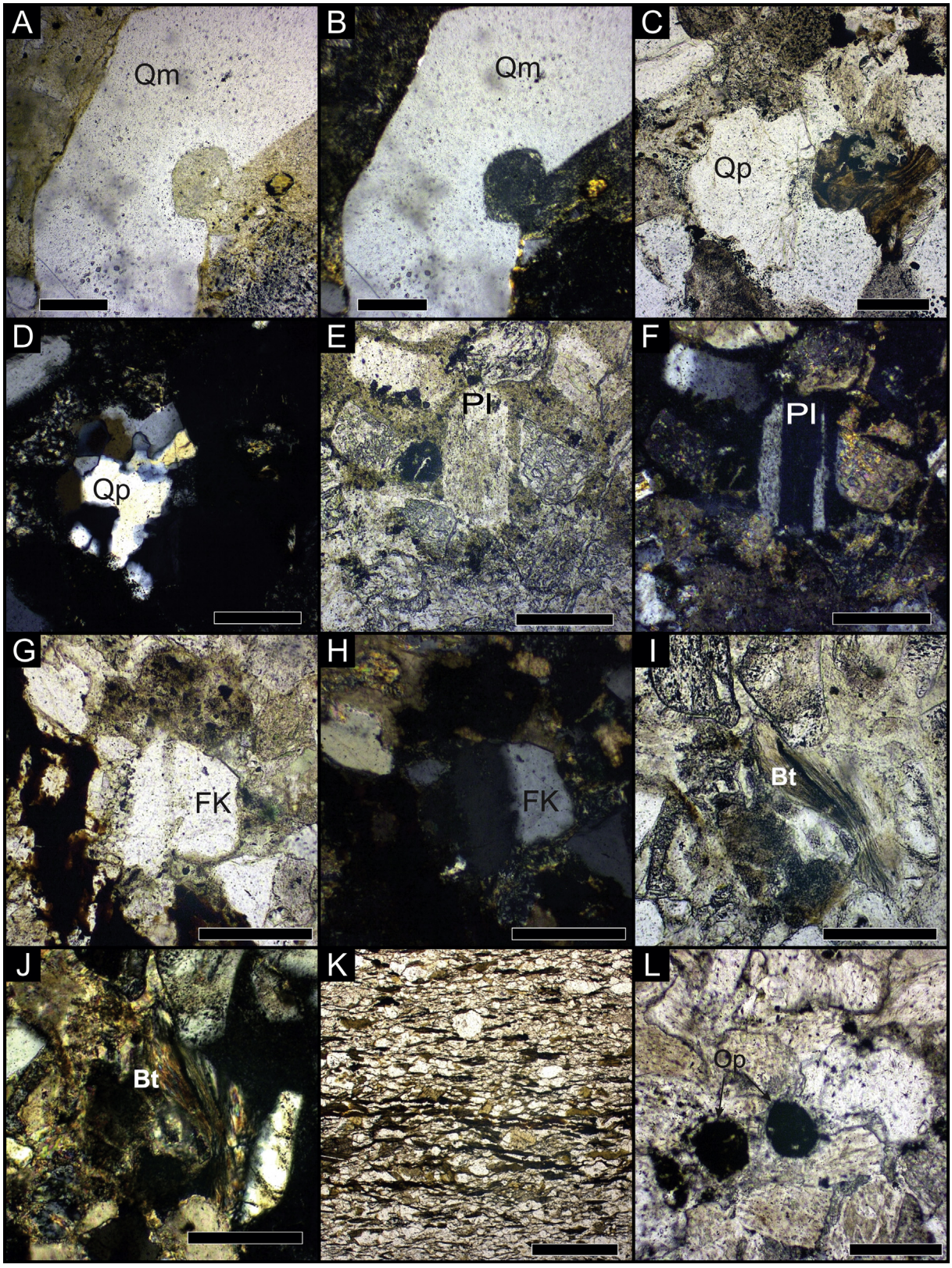

Fig. 10. Detrital components identified in sandstones thin sections. A–B. Monocrystalline quartz (Qm). C–D. Policrystalline quartz (Qp). E–F. Plagioclase (Pl). G–H. Potassic feldspar (FK). I–K. Biotite (Bt). L. Opaque minerals (Op). Photos A, C, E, G, I, K and L are without polarizer. Photos B, D, F, H and J with polarizer. Scale bar is 200 microns.

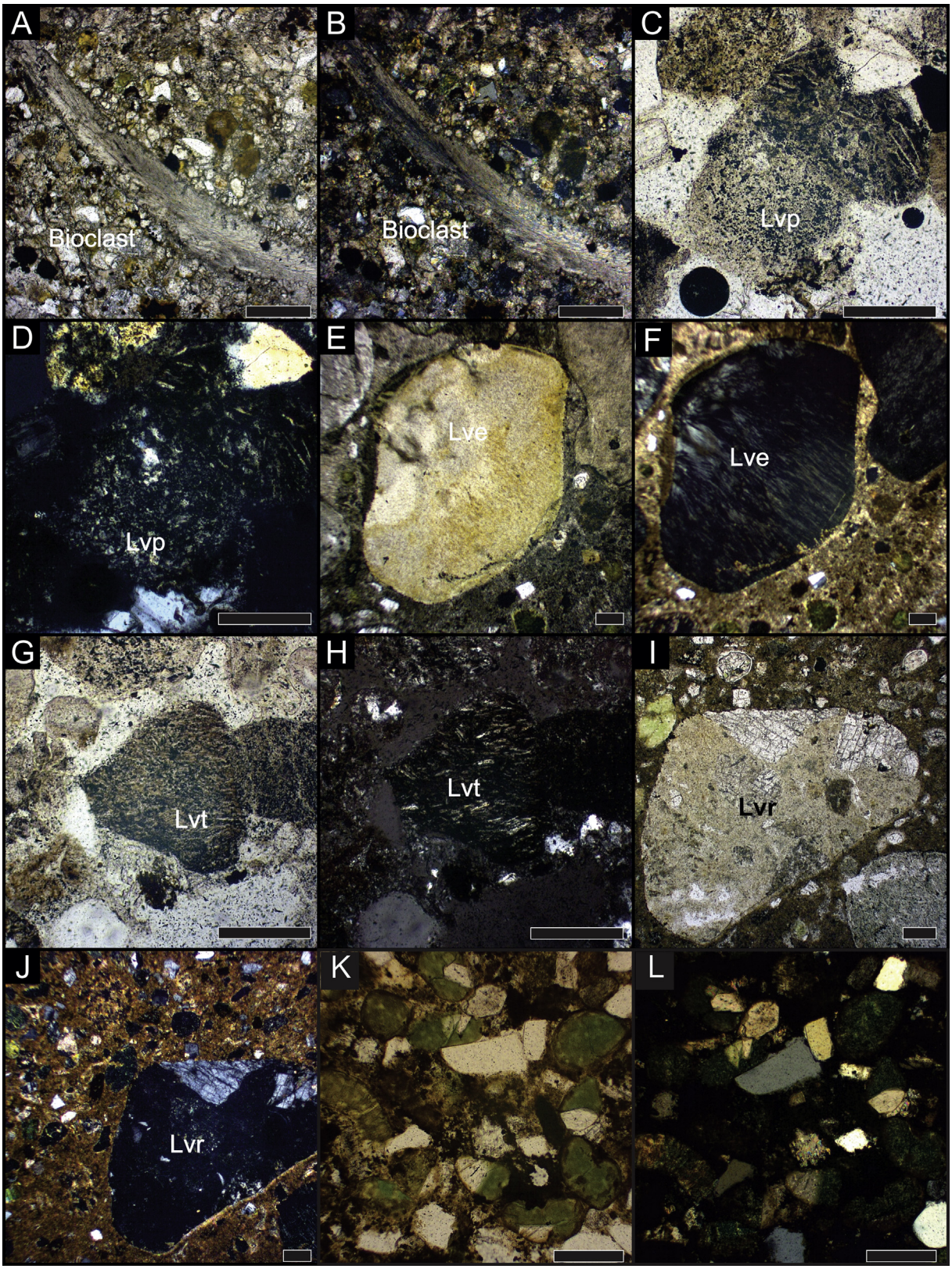

Fig. 11. Detrital components observed in sandstones thin sections. A–B. Bioclast. C-D. Volcanic lithic with pilotaxic texture (Lvp). E–F. Volcanic lithic with esferulitic texture (Lve). G-H. Volcanic lithic with traquitic texture (Lvt). I-J. Volcanic riolithic clast (Lvr). K–L. Glauconitic lithic (Lg). Photos A, C, E, G, I and K are without polarizer. Photos B, D, F, H, J and L with polarizer. Scale bar is 200 microns.

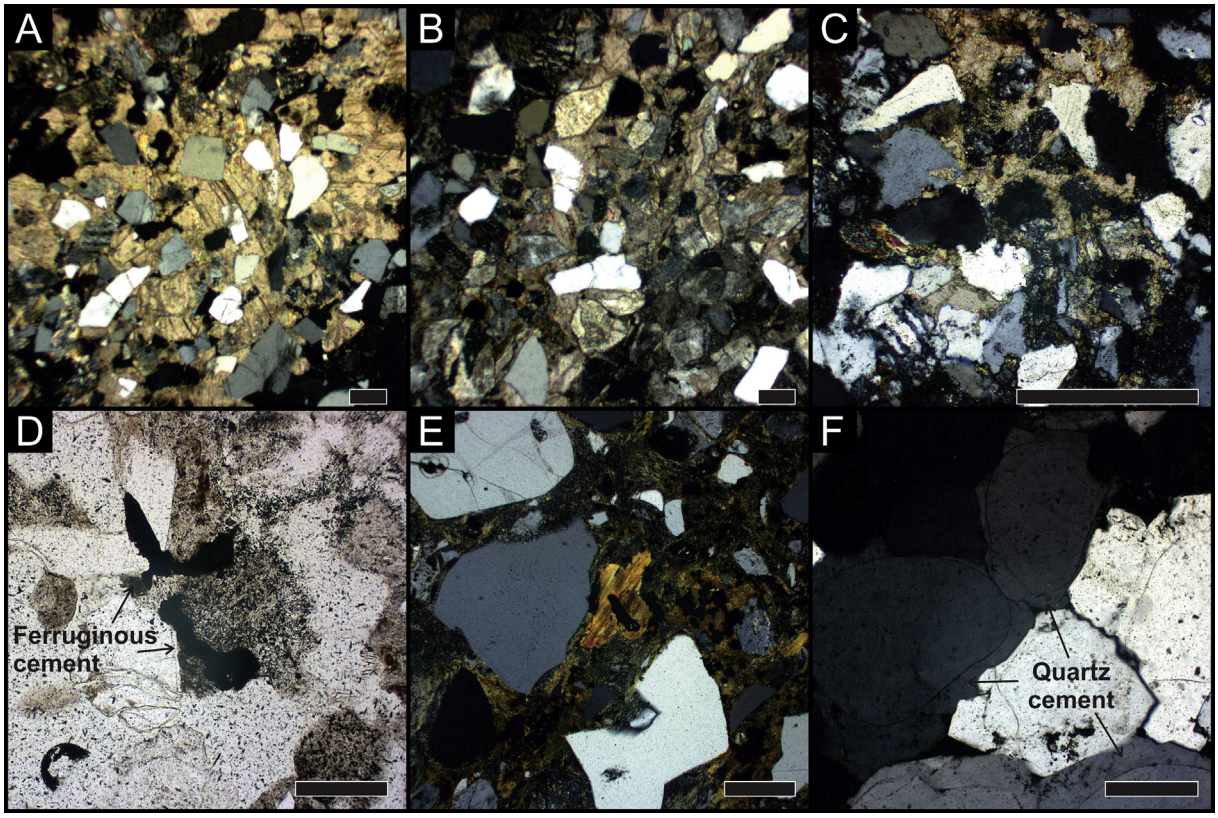

Fig. 12. Sandstone cements. A,B,C. Carbonate cements. D. Ferruginous cements. E. Argillic cement. F. Siliceous cement. Photo D without polarizer. Photos A, B, C, E and F with polarizer. Scale bar is 200 microns.

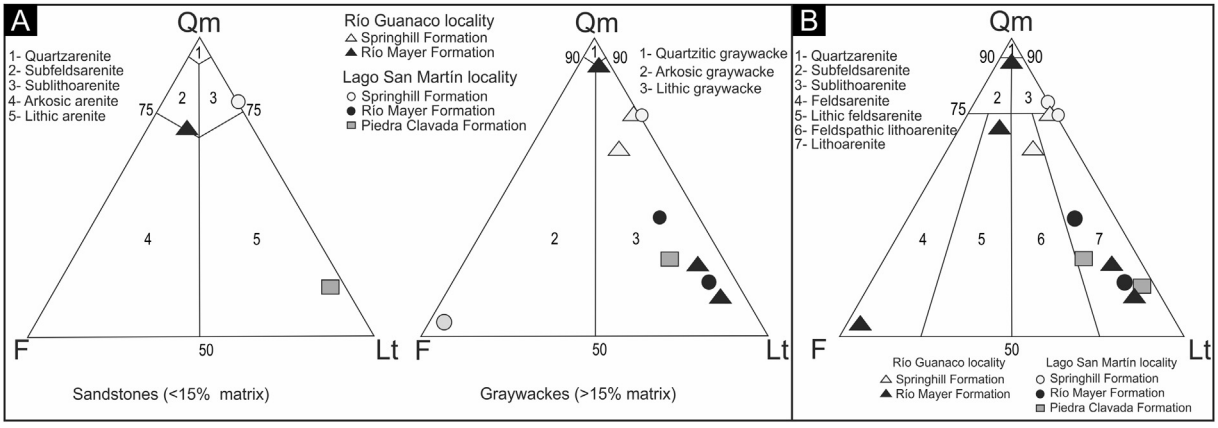

Fig. 13. Detrital modes of sandstones from Río Mayer Formation. A. Classical Qm-F.Lt diagram for sandstone classification taken from Dott, 1964 (modified for Pettijohn et al., 1972). B. Qm-F-Lt ternary diagram of Folk et al., 1970.

(51% in average) confirmed the increased vertical trend tendency initiated in assemblage C (Fig. 4; Table 3).

Transition from illite-rich shales of Río Mayer Formation from the lower section to chlorite-rich mudstones towards the upper section at Seccional Río Guanaco locality is clearly noticed in the clay assemblage ternary graph (Fig. 14) and in the areal distribution graph (Fig. 8).

As was observed in the Río Guanaco region, the Río Mayer Formation composition at Lago San Martín locality (Fig. 5; Table 4) contains variable proportions of quartz, feldspar, calcite, illite and IS, besides smectite (only in the transition towards the overlying Piedra Clavada Formation). Although detail analysis of this area are only complementary of the previous, four different compositional segments are clearly recognized (Fig. 5). The sample derived from Springhill Formation shows the higher kaolinite proportion (91%) which is practically absent in the rest of the samples (Fig. 5; Table 4). Profile 2 (PELF), entirely corresponding to marine deposits of Río Mayer Formation, can be divided in two segments according to its whole-rock composition. One characterized by high calcite participation (44% in average) with variable quartz (27.5%) and moderate feldspar (14.5%) and clays (11%) (Fig. 5; Table 4). The second segment with higher quartz contents (51% in average) but

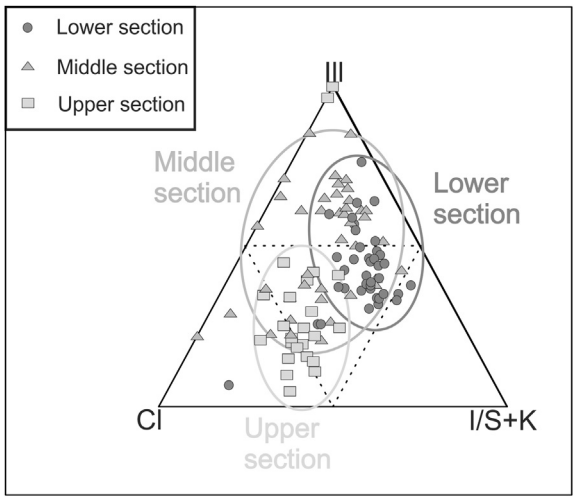

Fig. 14. Triangular compositional diagram of clays from Río Mayer Formation at Río Guanaco locality. Ill: illite; Cl: chlorite; IS: illite-smectite mixed layer; K: kaolinite.

with less noticeable in feldspar contents (7%; except for sample PEF20 with 40%) (Fig. 5; Table 4). The clay–mineral composition in the profile 2 shows the dominance of chlorite (46% in average). Finally, the transitional section to the overlaying Piedra Clavada Formation shows higher quartz proportions in whole-rock (64% in average) while in clay-fraction smectite prevails (97% in average) (Fig. 5; Table 4).

Results of clay-fraction analysis obtained for this unit are correlated with the clay zone C defined by Iñiguez Rodríguez and Decastelli (1984), where the authors mentioned the highest abundance of mixed-layered illite-smectite associated with chlorite. Río Mayer Formation outcrops display higher amounts of illite than documented on subsurface data. In turn this study confirmed the assumption of these authors that the diagenesis grade reached for this unit (based in mixed-clay expansive layers study) was an intermediate mesodiagenesis. The congruence between the results here presented and the data from the subsurface (using logs) is the evidence that the oil thermal maturity pattern presented for the Río Mayer Formation in the outcrops was reached before being uplifted. They also mentioned the presence of kaolinite in Springhill Formation and smectite prevalence in the Río Mayer Formation units (i.e. Piedra Clavada Formation). These results match with observed at Lago San Martín locality.

SEM-EDAX analyses allows to identify that most of the clays observed in the study units have a detrital origin, illite shows morphologies and dispositions that may indicate they were transported (Fig. 6A–B). The recognition of the $2M_1$ as the main polytype of illite (regarding the peaks of non-oriented clay-fraction XRD) (Fig. 7A), make possible to confirm its origin for this clay mineral.

On the other hand, Fe-rich chlorite recognized filling pores with moderate crystallinity growth (Fig. 6C), as well as IS in staggered arrangements according to a predominant orientation of the IS flakes in pores (Fig. 6D). In these cases it suggested that Cl as IS had an authigenic origin during burial diagenesis although the existence of detrital chlorite and IS may not be discarded.

7.2. Sandstone provenance analysis

Provenance analysis of sandstones from the Río Mayer, Springhill and Piedra Clavada Formations are shown in the traditional ternary graphs (QmFLt and QtFL of Dickinson and Suczek, 1979 and Dickinson et al., 1983). These methods are accepted and used by many authors (Suczek and Ingersoll, 1985; Packer and Ingersoll, 1986; Manassero, 1988), though they were also discussed by others (Ingersoll, 1990; Ingersoll et al., 1993; Critelli et al., 1997; Varela et al., 2013). Several factors as climate, agent of transport, distance to the source area, tectonic and subsidence of the basin controlled the distribution of detrital modes, and they also depend on the diagenetic processes (Dickinson and Suczek, 1979; Marsaglia and Ingersoll, 1992; Ingersoll et al., 1993; Gómez-Peral et al., 2011).

According to QmFLt diagram samples from the Springhill Formation are located in the field of quartzitic recycled orogen (Fig. 15A). The Río Mayer Formation samples present a more disperse distribution, for the Seccional Río Guanaco locality they are near the Qm-F line, corresponding to the interior craton, transitional continental and up-lift basement fields (Fig. 15A). On the other hand, samples of this units belonging from the Lago San Martín locality are mainly developed into the mixed and recycled orogen-transitional fields (Fig. 15A). Sandstones from the Piedra Clavada Formation are situated at the lithic recycled and transitional arc fields (Fig. 15A).

Taking into account the QtFL diagram the samples from the Springhill Formation are located in the recycled orogen and interior craton fields (Fig. 15B). For the Río Mayer Formation the recycled orogen prevail (4 samples), while in minor proportion the interior craton, transitional continental and up-lift basement are present (Fig. 15B). Finally, in the Piedra Clavada Formation one sample is plotted in the recycled orogen field and another one in the transitional arc field (Fig. 15b).

With regards to the sample distribution four different groups of samples were discriminated in the QmFLt diagram while three were identified in the QtFL diagram (Fig. 15). In this diagram is possible to establish a clear differentiation between two groups of samples, one pre-Aptian and one Aptian–Albian (Fig. 15A). In the pre-Aptian group there are two populations, the first one (A) is made by sandstones and graywackes from the middle and the beginning of the upper sections of the Río Mayer Formation at Seccional Río Guanaco locality (Fig. 15A). The second population (B) corresponds to four (4) samples of the Springhill Formation and the glauconitic sandstones of the initial Río Mayer Formation at Lago San Martín locality (Fig. 15A). Both populations are composed by more than 60% of monocrystalline quartz (Qm). The differentiation between these two populations is by the percentage of feldspars (F) and the lithics (Lt), which predominates in the population B (Table 5; Fig. 15A).

Since the Aptian there is registered an important change in the composition of the sandstones, generating two other populations (C and D), both with low percentage of Qm and high proportion of Lt + F (Fig. 15A). The first population (C) includes the prodelta samples of the Río Mayer Formation and two (2) samples of the deltaic Piedra Clavada Formation (Fig. 15A). Lastly, one sample recovered from the top of the Río Mayer Formation at Seccional Río Guanaco locality is considerably different to the others analysed, for this reason is considered one separated population (D), even when it has only one sample (Fig. 15A).

It is possible to determine two main controlling factors as the origin of the four populations identified: the percentage of volcanic lithics and the final depositional environment. The first one is the responsible for the differentiation in two major groups, the pre-Aptian and Aptian–Albian assemblages. The highest participation of volcanic lithics is registered at the north of the study area in the Río Mayer and Piedra Clavada Formations. Moreover, this is directly related to the increase in the proportion of feldspars observed by petrography and XRD. The second factor to be considered is the depositional palaeoenvironment, which generates the division of each major assemblage into two populations. In the pre-Aptian samples is possible to distinguish one population (B) that

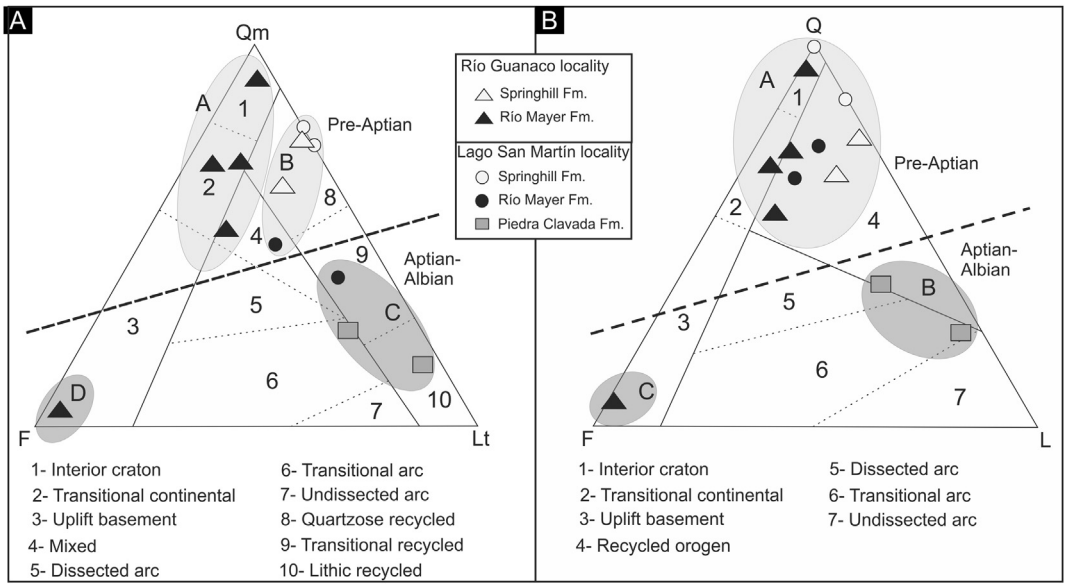

Fig. 15. Triangular diagram of provenance of sandstones from Río Mayer Formation. A. Provenance of the sandstone samples from the Río Mayer Formation in the Qm-F-Lt triangle. B. The same samples plotted into the Q-F-L diagram (After Dickinson et al., 1983).

correspond to the littoral marine palaeoenvironments and the other one is represented by the sandstones deposited by distal turbidity currents in a outer shelf palaeoenvironment (population A). Similar situation could be observed for the Aptian–Albian assemblage, due to the population C correspond to the prodelta and delta front samples while the population D is associated with the turbiditic deposits of the outer shelf palaeoenvironment.

A similar situation to the here described was observed in the Appalachian by Walker et al. (1994). These authors identified a compositional variation in the sandstones originated from the same source rock as a consequence of the different palaeogeographic position into the basin. In that study, the authors analysed both continental and marine sedimentary rocks developed in a transition between rifting and passive margin settings. Furthermore, the study documented the change from modal compositions represented in the recycled orogen and volcanic continental fields to temporarily coeval units plotted in the continental block. This transition records the movement from lithic sandstones to rich quartz-feldspar compositions as a result the effect of sediment transport (Walker et al., 1994).

The populations A and D may have evolved from the populations B and C respectively if it is considered the long distance of transport between the proximal and distal palaeoenvironments. This transport generates the concentration of cristaloclasts against the lithics (Fig. 15A), causing that the outer shelf sandstones have a continental block signature, while the inner shelf sandstones are related to recycled orogen and volcanic arc (Fig. 15A).

On the other hand, the QtFL diagram results less informative and

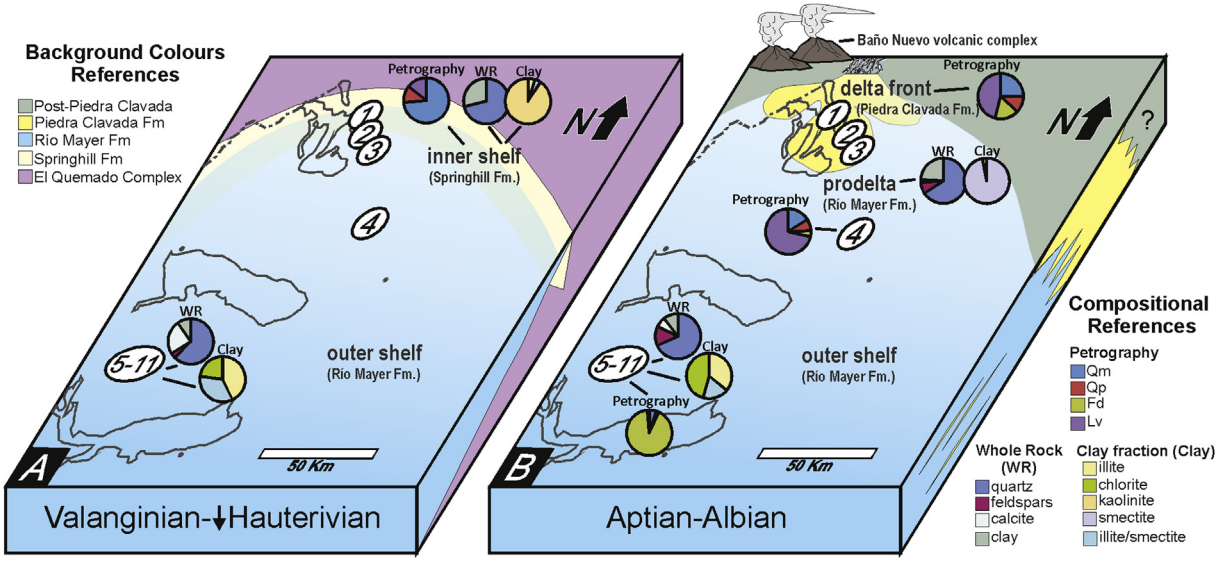

Fig. 16. Block diagram of the Austral Basin in the study area showing the compositional trend from inner (Springhill and Piedra Clavada Fms.) to outer (Río Mayer Fm.) shelf deposits at two different stages. A. Valanginian-Hauterivian context. B. Aptian–Albian context. WR: Whole rock from XRD; Clay: Clay content from XRD. 1–10: Sections recovered from the field as in Fig. 1.

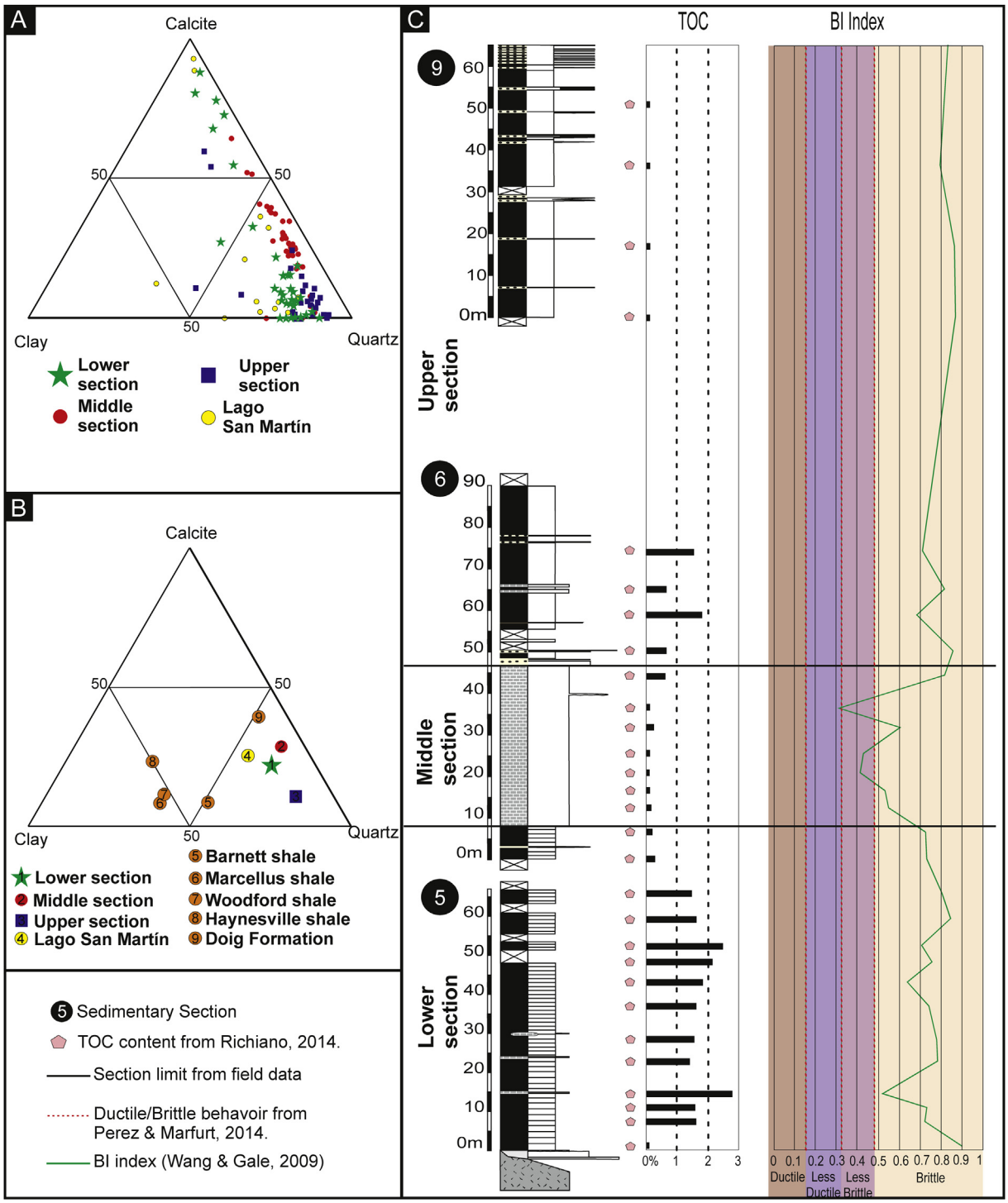

Fig. 17. Implicancies of the Río Mayer Formation composition in the hydrocarbon exploration of the Austral Basin. A. Ternary diagram (Calcite–Clay–Quartz) of the outcrops studied of the Río Mayer Formation. B. Comparison of the average compositional values from the Río Mayer Formation and some important shale reservoirs in North America (modified from Chalmers et al., 2012). 1–3 correspond to Río Guanaco locality. C. Wang and Gale (2009) brittleness index (BI) of the Río Mayer Formation in the Río Guanaco locality.

only registered three populations that partially match with the previous ones defined (Fig. 15B). The sample PEKA 20 (prodelta facies) is located in a different position than previously was, and now it is located between the pre-Aptian samples (population A). This population develops in the continental block and recycled orogen fields, but it is not clear a division between their samples (Fig. 15B). Finally, the populations B and C are equivalents to populations C and D respectively from the QmFLt diagram (Fig. 15).

The most conspicuous diagenetic component of the Río Mayer Formation is the pervasive calcite cement which produces irregular and corroded borders over the siliciclastic grains (Fig. 12C), this cement present poikilotopic texture in which crystals are anhedral and with sutured contacts. These features are in agreement with a deep burial stage (Fig. 12A–C; Flügel, 2004; Morad, 1998; among

Table 6
Brittleness index (BI) of the Río Mayer Formation in the Río Guanaco locality using Jarvie et al. (2007) and Wang and Gale (2009) indexes.

Río Mayer Formation							
Sample	Lithofacies	TOC %	Quartz	Calcite	Clay	BI index (Wang and Gale, 2009)	BI index (Jarvie et al., 2007)
IG 4	Shale	0.07	90	0	10	0.90	0.90
IG 9	Shale	1.59	72	9	17	0.72	0.73
IG 12	Shale	1.52	73	6	18	0.74	0.75
IG 17	Marl	2.81	52	32	14	0.52	0.53
IG 23	Shale	1.43	79	4	16	0.79	0.80
IG 27	Shale	1.56	78	4	16	0.78	0.80
IG 35	Shale	1.65	73	10	13	0.75	0.76
IG 38	Marly-mudstone	1.88	63	21	12	0.64	0.66
IG 39	Shale	2.09	77	0	22	0.76	0.78
IG 40	Shale	2.44	72	15	12	0.71	0.73
IG 42	Shale	1.59	85	2	11	0.85	0.87
IG 44	Shale	1.49	79	0	17	0.81	0.82
BP 1	Marly-mudstone	0.31	71	18	7	0.74	0.74
BP 5	Shale	0.17	71	15	11	0.73	0.73
PG 5	Marl	0.13	53	38	5	0.55	0.55
PG 9	Marl	0.09	51	38	6	0.54	0.54
PG 15	Marl	0.07	39	49	6	0.41	0.41
PG 19	Marl	0.09	42	50	5	0.43	0.43
PG 24	Marly-mudstone	0.17	58	26	10	0.62	0.62
PG 30	Marl	0.09	30	63	5	0.31	0.31
PG 35	Mudstone	0.58	74	7	8	0.83	0.83
PG 42	Mudstone	0.62	84	7	6	0.86	0.87
PG 50	Marly-mudstone	1.81	66	23	6	0.68	0.69
PG 55	Mudstone	0.6	70	5	9	0.83	0.83
PG 60	Marly-mudstone	1.48	65	16	9	0.71	0.72
PEVP1- 1	Mudstone	0.09	76	1	10	0.87	0.87
PEVP1- 6	Mudstone	0.09	78	5	7	0.87	0.87
PEVP1- 9	Mudstone	0.09	68	8	9	0.80	0.80
PEVP1- 14	Mudstone	0.09	74	6	8	0.84	0.84

others).

7.3. Regional implications of the compositional analysis

From the compositional analysis of the Río Mayer Formation in the Río Guanaco locality two independent sectors with different composition were identified. Firstly, during the Berriasian–Hauterivian (lower and middle sections) the unit presents in XRD high amounts of quartz and illite associated with low proportion of feldspars (Fig. 16A). Secondly, during the Hauterivian–Albian (the last five meters of the middle section and the entire upper section) the Río Mayer Formation shows in the XRD an increase in feldspar content and the chlorite occur in higher proportions; while feldspars and volcanic lithics are present in the sandstones (Fig. 16B). All of these changes are slightly noticed in the Valanginian-Hauterivian but they are clearly identified in the Aptian–Albian (Fig. 16).

The transition between the Río Mayer and Piedra Clavada formations in the northern region (Lago Viedma- Lago San Martín localities) is characterized by high amounts of volcanic lithics (Fig. 16B). This situation is correlated with the increase in feldspars in the Seccional Río Guanaco locality during the Aptian–Albian (Fig. 16B). The volcanic lithics recovered at Estancia La Vega locality (Fig. 1), display many feldspar phenocrystals, many of which are unaltered (very well preserved) and they are up to 10 times the size of the feldspars found in graywackes from the Seccional Río Guanaco locality. Due to weathering and transport which have been exposed near the edge of basin sediments, evolution would favour the freedom of such phenocrystals, which subsequently deposited, with very small sizes, about 85 km towards the south in the upper section of the Río Mayer Formation at Seccional Río Guanaco locality (Fig 16B).

Furthermore, the exclusive participation of S_a assemblage in fine-grained sediments and volcanic components in sandstones and graywackes from the Río Mayer Formation at Lago San Martin locality with respect to samples of the same age in the Seccional Río Guanaco locality are related to the development of the volcanic arc proposed for the Neocomian, which was located at the north (latitude 47° S) and corresponds to the early stage of the Austral Patagonian Batholith (Ramos et al., 1982; Suárez et al., 2010) (Fig. 16B). This arc was called Baño Nuevo Volcanic Complex, developed from the Hauterivian to early Aptian, and consists of tuffs associated with surtseyans eruptions (Suárez et al., 2010).

Different lines of evidence suggest that the deposition of the Río Mayer Formation was coeval with the development of a volcanic arc at least from the Valanginian. This volcanic arc had the most influence on the unit in the northern region of the study area (Lago San Martín locality) compared with the Seccional Río Guanaco locality at the south.

7.4. Applicability of the compositional analyses in unconventional reservoir characterization

The composition of sedimentary rocks has generated great interest in recent studies of black shales reservoirs. In this regard, most of the successful shale plays are mostly composed of quartz and carbonate minerals that create the conditions required for brittle exploitation (Binnion, 2012). A mineralogical composition mainly composed by quartz, calcite and feldspars promotes brittleness in the rock, while clay minerals, in general terms, tend to facilitate ductile behaviour (Binnion, 2012). The Río Mayer Formation is almost entirely composed by quartz and calcite, with low proportion of clays (Fig. 17A). Compared with one of the most famous shale-gas in the world, the Barnett shale, the Río Mayer Formation has a composition richer in quartz and calcite than the reservoir mention. Moreover, in comparison with other important shale-reservoirs from North America (Barnett, Marcellus, Woodford, Haynesville and Doig; Fig. 17B), the compositional average

values of the unit studied have better (more quartzitic) composition. This aspect is very important for the brittleness behaviour of the rocks. In this sense, applying the brittleness index (BI) proposed by Jarvie et al. (2007) and Wang and Gale (2009) the samples of the Río Mayer Formation from the Seccional Río Guanaco locality shows a clear brittle pattern according to Perez and Marfurt (2014) classification (Fig. 17C, Table 6).

In general, a good approach to understand the mudrock system is to develop a shelf-to-basin transect (similar to the presented in this study), in order to determine the best facies for reservoir development (Hammes and Frébourg, 2012). Best shale-gas reservoirs were deposited distal, low-oxygenated, high-organic low-clay settings (Hill et al., 2007; Loucks and Ruppel, 2007; Hammes and Frébourg, 2012).

One important topic to be considered for future studies in this region of South America is the relationship between diagenetic processes and natural fractures. In this regard, recent studies have focused on modelling target shales from analogue field data or theoretical models to evaluate the possibility of predicting the distribution of fractures (Gale et al., 2007). If shear fracturing due to diagenesis has occurred, it can fundamentally alter the magnitude and anisotropy of permeability in these low permeability sediments (Cartwright, 2011).

The composition of the Río Mayer Formation in the study area highly matches with the requirements to be considered for shale-oil/gas exploration. In this respect, the lower section of the unit is the interval that has reservoir potential because of the excellent compositional qualities and high TOC values. The long transport suffered by the sediments from the littoral to the outer shelf in a trangressive context, together with an interplay between anoxic conditions and low sedimentation rates (Richiano, 2015) generates that the deposits recovered at the lower section of the unit at Seccional Río Guanaco locality comprise the best potential play to be wanted in the subsurface.

8. Conclusions

XRD analyzes of whole rock from the Río Mayer Formation in the study area indicate a composition dominated by quartz and calcite, with minor amounts of feldspar and clay minerals. The clay-fraction shows a shift from illite-dominated to chlorite-dominated sectors in the marine sedimentary environment. In the prodelta facies smectite dominates over 90%. Authigenic clays and detrital origin were identified using SEM-EDAX and standard petrography. The fine sediments were grouped into four clay assemblages (I, IS, Cl, Sm), which are distributed with a clear pattern of both stratigraphic and areal arrangement.

From a petrographic point of view, sandstones of the Río Mayer Formation are mostly feldspathic or lithic graywackes. Respect to their provenance, taking into account the Qm-F-Lt diagram four populations were defined, two corresponding to the pre-Aptian deposits and two from the Aptian–Albian assemblages. The compositional differences found in each temporal group are attributed to changes in palaeoenvironments where rocks finally were deposited. Thus, the sediments carried in the inner shelf correspond with a recycling orogen and volcanic arc, while samples developed by turbidity currents deposited in the outer shelf are from a continental block field. The Río Mayer Formation in the Seccional Río Guanaco locality displays more stable components than contemporaneous rocks at Lago San Martín locality. Such variation is explained by the concentration of stable crystalline clasts as a consequence of a selective transport from the proximal to distal environments.

The sediment contribution during the sedimentation of the Río Mayer Formation was clearly influenced by volcanic activity in the arc associated with the Southern Patagonian Batholith. The pattern observed in the plutonic/volcanic development related to this batholith left its stamp on the mineralogical composition of the rocks of the unit analysed.

Finally, the Río Mayer Formation possesses all the attributes needed to enter in the new exploration horizon: Unconventional Hydrocarbon Reservoirs. The contents of TOC, the compositional aspects (mineralogy and BI), the degree of diagenesis reached, the thickness and areal distribution of the focused facies make this unit as a very conducive to the search of new hydrocarbon reserves in the Austral Basin.

Acknowledgements

We would like to thank to P. Desjardins and the associated editor L. Buatois whose useful comments and observations improved the quality of the manuscript. This study was supported by grants from CONICET (PIP1016/10), Agencia Nacional de Promoción Científica y Tecnológica (PICT 2013-1298) and Programa de Incentivos (Universidad Nacional de La Plata, N11-633). The authors deeply thanks to the Los Glaciares National Park for the field assistance, to B. Aguirre-Urreta for the determination of the fossil material. We would like to thank to C. Genazzini and P. Garcia for their help in XRD analysis, to D. Mártire and M. Pousada for the preparation of thin-sections and to A. Cerlani for his technical assistance in the SEM-EDAX analysis.

References

Aguirre Urreta, M.B., 2002. Invertebrados del cretácico inferior. In: Haller, M.J. (Ed.), Geología y Recursos Naturales de Santa Cruz. Relatorio del Decimoquinto Congreso Geológico Argentino, 925 pp.
Allen, P.A., Mange-Rajetzky, M.A., 1992. Devonian-carboniferous sedimentary evolution of the Clair area, offshore north-western UK: impact of changing provenance. Mar. Pet. Geol. 9, 29–52.
Amorosi, A., 1995. Glaucony and sequence stratigraphy: a conceptual framework of distribution in siliciclastic sequences. J. Sediment. Res. 65, 419–425.
Amorosi, A., 1997. Detecting compositional, spatial, and temporal attributes of glaucony: a tool for provenance research. Sediment. Geol. 109, 135–153.
Arbe, H., Hechem, J., 1984. Estratigrafía y facies de depósitos continentales, litorales y marinos del Cretácico superior, lago Argentino. IX Congr. Geol. Argent. Actas 7, 124–158.
Arbe, H.A., 2002. Análisis estratigráfico del Cretácico de la Cuenca Austral. In: Haller, M.J. (Ed.), Geología y Recursos Naturales de Santa Cruz. Relatorio del XV Congreso Geológico Argentino, pp. 103–128.
Argüello, J., Trapiche, A., Berdini, O., Pedrazzini, M., Benotti, S., 2005. Entrampamiento de petróleo y gas en la Formación Springhill, sector continental de la Cuenca Austral, República Argentina. In: Trampas de Hidrocarburos en las Cuencas Productivas de Argentina, VI Congreso de Exploración y Desarrollo de Hidrocarburos.
Belotti, H., Pagan, F., Perez Mazas, A., Agüera, M., Rodriguez, J., Porras, J., Köhler, G., Weiner, G., Conforto, G., Cagnolatti, M., 2013. Geologic interpretation and assessment of early cretaceous shale oil and Gas potential in austral Basin, Santa Cruz, Argentina. In: Unconventional Resources Technology Conference, Denver, Colorado, USA, August 2013.
Best, M.G., Christiansen, E.H., 2001. Igneous Petrology. Blackwell Science, Oxford.
Biddle, K., Uliana, M., Mitchum Jr., R., Fitzgerald, M., Wright, R., 1986. The stratigraphic and structural evolution of central and eastern Magallanes Basin, Southern America. In: Allen, P.A., Homewood, P. (Eds.), Foreland Basins, International Association of Sedimentologist Special Publication, 8, pp. 41–61.
Binnion, M., 2012. How the technical differences between shale gas and conventional gas projects lead to a new business model being required to be successful. Mar. Pet. Geol. 31, 3–7.
Biscaye, P.E., 1965. Mineralogy and sedimentation of recent deep sea clay in the Atlantic Ocean and adjacent seas and oceans. Geol. Soc. Am. Bull. 76, 803–832.
Brown, G., Brindley, G.W., 1980. X-ray diffraction procedures for clay mineral identification. In: Brindley, G.W., Brown, G. (Eds.), Crystal structures of Clay Minerals and Their X-ray Identification. Mineralogical Society, London, pp. 305–359.
Cartwright, J., 2011. Diagenetically induced shear failure of fine-grained sediments and the development of polygonal fault systems. Mar. Pet. Geol. 28, 1593–1610.
Cavazza, W., Ingersoll, R.V., 2005. Detritical modes of the Ionian Forearc Basin fill (Oligocene-Quaternary) reflect the tectonic evolution of the Calabria-Peloritani Terrane (Southern Italy). J. Sediment. Res. 15, 268–279.
Chalmers, G.R., Bustin, R.M., Power, I.M., 2012. Characterization of gas shale pore systems by porosimetry, pycnometry, surface area, and field emission scanning

electron microscopy/transmission electron microscopy image analyses: examples from the Barnett, Woodford, Haynesville, Marcellus, and Doig units. AAPG Bull. 96, 1099–1119.
Critelli, S., Ingersoll, R.V., 1995. Interpretation of neovolcanic versus paleovolcanic sand grains: an example from Miocene deep marine sandstones of the Topanga Group (Southern California). Sedimentology 42, 783–804.
Critelli, S., Le Pera, E., Ingersoll, R.V., 1997. The effects of source lithology, transport, deposition and sampling scale on the composition of southern California sand. Sedimentology 44, 653–671.
De Rossi Fontanelli, P., De Ros, L.F., Dorneles Remus, M.V., 2012. Provenance of deep-water reservoir sandstones from the Jubarte oil field, Campos Basin, Eastern Brazilian Margin. Mar. Pet. Geol. 26, 1274–1298.
Dickinson, W.R., Rich, E.I., 1972. Petrologic intervals and petrofacies in the great Valley sequence, Sacramento Valley, California. Geol. Soc. Am. Bull. 83, 3007–3024.
Dickinson, W.R., Suczek, C., 1979. Plate tectonics and sandstone composition. Am. Assoc. Pet. Geol. Bull. 63, 2164–2182.
Dickinson, W.R., Beard, L.S., Brakenridge, G.R., Erjavec, J.L., Ferguson, R.C., Inman, K.F., Knepp, R.A., Lindberg, F.A., Ryberg, P.T., 1983. Provenance of North American Phanerozoic sandstones in relation to tectonic setting. Geol. Soc. Am. Bull. 94, 222–235.
Do Campo, M., Del Papa, C., Nieto, F., Hongn, F., Petrinovic, I., 2010. Integrated analysis for constraining palaeoclimatic and volcanic influences on clay–mineral assemblages in orogenic basins (Palaeogene Andean foreland, Northwestern Argentina). Sediment. Geol. 228, 98–112.
Dott, R.H., 1964. Wacke, greywacke and matrix-what approach to immature sandstone classification? J. Sediment. Petrol. 34, 625–632.
Fildani, A., Cope, T., Graham, S., Wooden, J., 2003. Initiation of the Magallanes foreland basin: timing of the southernmost Patagonian Andes orogeny revised by detrital circon provenance analysis. Geology 31, 1081–1084.
Fildani, A., Hessler, A., 2005. Stratigraphic record across a retroarc basin inversion: rocas Verdes–Magallanes Basin, patagonian Andes, Chile. GSA Bull. 117, 1596–1614.
Flügel, E., 2004. Microfacies of Carbonate Rocks: Analysis, Interpretation and Application. Springer, Berlin, Heidelberg, New York.
Folk, R.L., Andrews, P.B., Lewis, D.W., 1970. Detrital sedimentary rock classification and nomenclature for use in New Zealand. N. Z. J. Geol. Geophys. 13, 937–968.
Fosdick, J.C., Romans, B.W., Fildani, A., Bernhardt, A., Calderón, M., Graham, S.A., 2011. Kinematic evolution of the Patagonian retroarc fold-and-thrust belt and Magallanes foreland basin, Chile and Argentina, 51°30'S. Geol. Soc. Am. Bull. 123, 679–698.
Gale, J.F., Reed, R.M., Holder, J., 2007. Natural fractures in the Barnett Shale and their importance for hydraulic fracture treatments. AAPG Bull. 91, 603–622.
Gómez-Peral, L.E., Raigemborn, M.S., Poiré, D.G., 2011. Petrología y evolución diagenética de las facies silicoclásticas del Grupo Sierras Bayas, Sistema de Tandilia, Argentina. Lat. Am. J. Sedimentol. Basin Anal. 18, 3–41.
Hammes, U., Frébourg, G., 2012. Haynesville and Bossier mudrocks: a facies and sequence stratigraphic investigation, East Texas and Louisiana, USA. Mar. Pet. Geol. 31, 8–26.
Hill, R.J., Jarvie, D.M., Zumberge, J., Henry, M., Pollastro, R.M., 2007. Oil and gas geochemistry and petroleum systems of the Fort Worth Basin. AAPG Bull. 91, 445–473.
Hurst, A., Morton, A.C., 1988. An application of heavy-mineral analysis to lithostratigraphy and reservoir modelling in the Oseberg Field, northern North Sea. Mar. Pet. Geol. 5, 157–169.
Ingersoll, R.V., 1983. Petrofacies and provenance of late Mesozoic Forearc Basin, northern and Central California. Am. Assoc. Pet. Geol. Bull. 67, 1125–1142.
Ingersoll, R.V., 1990. Actualistic sandstone petrofacies: discriminating modern and ancient source rocks. Geology 18, 733–736.
Ingersoll, R.V., Bullard, T.F., Ford, R.L., Grimm, J.P., Picke, J.D., Sares, S.W., 1984. The effect of grain size on detrital modes: a test of the Gazzi-Dickinson point-counting method. J. Sediment. Petrol. 54, 103–116.
Ingersoll, R.V., Kretchmer, A.G., Valles, P.K., 1993. The effect of sampling scale on actualistic sandstone petrofacies. Sedimentology 40, 937–953.
Inglès, M., Ramos-Guerrero, E., 1995. Sedimentological control on the clay mineral distribution in the marine and non-marine Palaeogene deposits of Mallorca (Western Mediterranean). Sediment. Geol. 94, 229–243.
Iñiguez Rodríguez, A.M., Decastelli, O.O., 1984. Mineralogía y diagénesis de arcillas de las Formaciones Cretácico-Terciarias de la Cuenca Austral. IX Congreso Geológico Argentino. Actas 3, 402–414.
Jarvie, D.M., Hill, R.J., Ruble, T.E., Pollastro, R.M., 2007. Unconventional shale-gas systems: the Mississippian Barnett Shale of North-Central Texas as one model for thermogenic shale-gas assessment. AAPG Bull. 91, 475–499.
Kohl, D., Slingerland, R., Arthur, M., Bracht, R., Engelder, T., 2014. Sequence stratigraphy and depositional environments of the Shamokin (Union Springs) Member, Marcellus Formation, and associated strata in the middle Appalachian Basin. AAPG Bull. 98, 483–513.
Kraemer, P.E., Riccardi, A.C., 1997. Estratigrafía de la región comprendida entre los lagos Argentino y Viedma (49° 40′–50° 10′ LS), Provincia de Santa Cruz. Rev. Asoc. Argent. Geol. 52, 333–360.
Kubler, B., 1966. La cristallinité de l'illite et les zonestout-a-faitsupéreures du metamorphisme. Colloq. étagestectoniques, Nêuchatel 105–122.
Legarreta, L., Villar, H., 2011. Geological and Geochemical Keys of the Potential Shale Resources, Argentina Basins. AAPG Geoscience Technology Workshop, Buenos Aires, pp. 1–21.
Loucks, R.G., Ruppel, S.C., 2007. Mississippian Barnett shale: lithofacies and depositional setting of a deep-water shale-gas succession in the Fort Worth Basin, Texas. AAPG Bull. 91, 579–601.
Lundegard, P.D., Samuels, N.D., 1980. Field classification of fine-grained sedimentary rocks. J. Sediment. Petrol. 50, 781–786.
Macellari, C.E., Barrio, C.A., Manassero, M.J., 1989. Upper Cretaceous to Paleocene depositional sequences and sandstone petrography of southwestern Patagonia (Argentina and Chile). J. S. Am. Earth Sci. 2, 233–239.
Manassero, M.J., 1988. Petrología y procedencia de las areniscas cretácicas superiores de la Cuenca Austral Argentina. Rev. Asoc. Geol. Argent. 18, 175–187.
Marinelli, R.V., 1998. Reservorios deltaicos de la Formación Piedra Clavada. Bol. Inf. Pet. 15, 28–37.
Marsaglia, K., Ingersoll, R., 1992. Compositional trends in arc-related, deep marine sand and sandstone: a reassessment of magmatic provenance. Geol. Soc. Am. Bull. 104, 1637–1649.
Mearns, E.W., 1992. Samarium-neodymium isotopic constraints on the provenance of the Brent Group. In: Morton, A.C., Haszeldine, R.S., Giles, M.R., Brown, S. (Eds.), Geology of the Brent Group. Geological Society Special Publication, vol. 61, pp. 213–225.
Moore, D.M., Reynolds Jr., R.C., 1997. X-ray Diffraction and the Identification and Analysis of Clay Minerals. Oxford University Press, Oxford.
Morad, S., 1998. Carbonate cementation in sandstones. In: Morad, Sadoon (Ed.), International Association of Sedimentologists Special Publication, 26.
Morton, A.C., 1987. Detrital garnets as provenance and correlation indicators in North Sea reservoir sandstones. In: Brooks, J., Glennie, K. (Eds.), Petroleum Geology of North West Europe. Graham and Trotman, London, pp. 991–995.
Morton, A.C., Hallsworth, C., 1994. Identifying provenance-specfic features of detrital heavy mineral assemblages in sandstones. Sediment. Geol. 90, 241–256.
Morton, A.C., Knox'B, R.W.O., Hallsworth, C., 2002. Correlation of reservoir sandstones using quantitative heavy mineral analysis. Pet. Geosci. 8, 251–262.
Morton, A.C., Spicer, P., Ewen, D., 2003. Geosteering of high-angle wells using heavy-mineral analysis: the Clair Field, West of Shetland, U.K. In: Carr, T.R., Mason, E.P., Feazel, C.T. (Eds.), Horizontal Wells: Focus on the Reservoir. AAPG Methods in Exploration 14, pp. 249–260.
Morton, A.C., Whitham, A.G., Fanning, C.M., 2005. Provenance of Late Cretaceous to Paleocene submarine fan sandstones in the Norwegian Sea: integration of heavy mineral, mineral chemical and zircon age data. Sediment. Geol. 182, 3–28.
Packer, B.M., Ingersoll, R.V., 1986. Provenance and petrology of Deep Sea Drilling Project sands and sandstones from the Japan and Mariana Forearc and backarc basins. Sediment. Geol. 51, 5–28.
Pankhurst, R.J., Riley, T.R., Fanning, C.M., Kelley, S.P., 2000. Episodic silicic volcanism in Patagonia and Antarctic Peninsula: chronology of magmatism associated with the break-up of Gondwana. J. Petrol. 41, 605–625.
Perez, R., Marfurt, K., 2014. Mineralogy-based brittleness prediction from surface seismic data: application to the Barnett Shale. Interpretation 2, 1–17.
Pettijohn, F.J., Potter, P.E., Siever, R., 1972. Sand and Sandstone. Springer, New York.
Pierce, J.W., Siegel, F.R., 1969. Quantification in clay mineral studies of sediments and sedimentary rocks. J. Sediment. Petrol. 39, 187–193.
Pittion, J.L., Gouadain, J., 1992. Source-rock and oil generation in the Austral Basin. In: 13 World Petroleum Congress, Buenos Aires, Proceedings, vol. 2, pp. 113–120.
Pittion, J.L., Arbe, H.A., 1999. Sistemas petroleros de la Cuenca Austral. In: IV Congreso de Exploración y Desarrollo de Hidrocarburos, Mar del Plata, pp. 239–262.
Potter, P.E., Maynard, J.B., Depetris, P.J., 2005. Mud and Mudstones, Introduction and Overview. Springer, Berlin.
Ramos, V.A., Niemeyer, H., Skarmeta, J., Muñoz, J., 1982. Magmatic evolution of the austral patagonian Andes. Earth-Sci. Rev. 18, 411–443.
Riccardi, A.C., 1968. Estratigrafía de la región oriental de la Bahía de la Lancha, Lago San Martín, Santa Cruz. Universidad Nacional de La Plata (PhD thesis).
Riccardi, A.C., 1971. Estratigrafía en el oriente de la Bahía de la Lancha, Lago San Martín, Santa Cruz, Argentina. Revista del Museo de la Plata. Sección Geol. 7, 245–318.
Riccardi, A.C., Rolleri, E.O., 1980. Cordillera Patagónica austral. Simp. Geol. Reg. Argent. 2, 1173–1304.
Richiano, S., 2012. Sedimentología e Icnología de la Formación Río Mayer, Provincia de Santa Cruz Argentina. Universidad Nacional de La Plata (PhD thesis).
Richiano, S., 2014. Lower cretaceous anoxic conditions in the austral Basin, southwestern Gondwana, patagonia Argentina. J. S. Am. Earth Sci. 54, 37–46.
Richiano, S., 2015. Environmental factors affecting the development of the *Zoophycos* ichnofacies in the Lower Cretaceous Río Mayer Formation (Austral Basin, Patagonia). Palaeogeogr. Palaeoclimatol. Palaeoecol. http://dx.doi.org/10.1016/j.palaeo.2015.03.029.
Richiano, S., Varela, A.N., Cereceda, A., Poiré, D.G., 2012. Evolución paleoambiental de la Formación Río Mayer, Cretácico inferior, Cuenca Austral, Patagonia Argentina. Lat. Am. J. Sedimentol. Basin Anal. 19, 3–26.
Richiano, S., Poiré, D.G., Varela, A.N., 2013. Icnología de La Formación río Mayer, cretácico inferior, so Gondwana, Patagonia, Argentina. Ameghiniana 50, 273–286.
Rodríguez, J., Miller, M., 2005. Cuenca Austral. Frontera Exploratoria de la Argentina. In: VI Congreso de Exploración y Desarrollo de Hidrocarburos, pp. 308–323.
Rodríguez, J.F., Cagnolatti, M.J., 2008. Source Rocks and Paleogeography, Austral Basin, Argentina. AAPG Convention, San Antonio, TX.

Rossi, C., Kälin, O., Arribas, J., Tortosa, A., 2002. Diagenesis, provenance and reservoir quality of Triassic TAGI sandstones from Ourhoudfield, Berkine (Ghadames) Basin, Algeria. Mar. Pet. Geol. 19, 117–142.
Schultz, L.G., 1964. Quantitative interpretation of mineralogical composition from X-ray and chemical data for Pierra Shale. In: U.S. Geological Survey Professional Paper, vol. 391, pp. 1–31.
Spalletti, L.A., Franzese, J.R., 2007. Mesozoic Paleogeography and Paleoenvironmental evolution of Patagonia (Southern South America). In: Gasparini, Z., Salgado, L., y Coria, R.A. (Eds.), Patagonian Mesozoic Reptiles. Indiana University Press, Bloomington & Indianapolis, pp. 29–49.
Spalletti, L.A., Matheos, S.D., Sanchez, E., Oyarzábal, F., 2006. Análisis diagenético de la Formación Springhill (Santa Cruz, Argentina). Boletin de Informaciones Petroleras, pp. 60–73.
Suárez, M., Demant, A., De La Cruz, R., Fanning, M., 2010. 40Ar/39Ar and U–Pb SHRIMP dating of Aptian tuff cones in the Aisén Basin, Central Patagonian Cordillera. J. S. Am. Earth Sci. 29, 731–737.
Suczek, C.A., Ingersoll, R.A., 1985. Petrology and provenance of Cenozoic sand from the Indus cone and Arabian basin, DSDP sites 221, 222 and 224. J. Sediment. Petrol. 55, 340–346.
Varela, A.N., 2011. Sedimentología Y Modelos Deposicionales De La Formación Mata Amarilla, Cretácico De La Cuenca Austral, Argentina. Universidad Nacional de La Plata (PhD thesis).
Varela, A.N., Poiré, D.G., Martin, T., Gerdes, A., Goin, F.J., Gelfo, J.N., Hoffmann, S., 2012. U-Pb zircon constraints on the age of the Cretaceous Mata Amarilla Formation, Southern Patagonia, Argentina: its relationship with the evolution of the Austral Basin. Andean Geol. 39, 359–379.
Varela, A.N., Gómez Peral, L.E., Richiano, S., Poiré, D.G., 2013. Distinguishing similar volcanic source areas from an integrated provenance analysis: implications for foreland Andean basins. J. Sediment. Res. 83, 258–276.
Walker, D., Simpson, E.L., Driese, S.G., 1994. Paleogeographic influences on sandstone composition along an evolving passive margin; an example from the basal Chilhowee Group (uppermost Proterozoic to Lower Cambrian) of the south-central Appalachians. J. Sediment. Res. 64, 807–814.
Wang, F.P., Gale, J.F.W., 2009. Screening criteria for shale-gas systems. Gulf Coast Assoc. Geol. Soc. Trans. 59, 779–793.
Warr, L.N., Rice, A.H.N., 1994. Interlaboratory standardization and calibration of clay mineral crystallinity and crystallite size data. J. Metamorph. Geol. 12, 141–152.
Wilson, T.J., 1991. Transition from back-arc to foreland basin development in southernmost Andes: stratigraphic record from the Ultima Esperanza District, Chile. Geol. Soc. Am. Bull. 103, 98–111.
Zanella, A., Cobbold, P.R., Rojas, L., 2013. Beef veins and thrust detachments in Early Cretaceous source rocks, foothills of Magallanes-Austral Basin, southern Chile and Argentina: structural evidence for fluid overpressure during hydrocarbon maturation. Mar. Pet. Geol. 55, 250–261.